Tunnel Boring Machine (TBM) Performance in Singapore's Mass Rapid Transit (MRT) system

by

Wanling Chong
B.Eng. Civil Engineering
Nanyang Technological University, Singapore
(2012)

Submitted to the Department of Civil and Environmental Engineering in partial fulfillment of the requirements for the degree of

Master of Engineering in Civil and Environmental Engineering

at the

MASSACHUSETTS INSTITUTE OF TECHNOLOGY
June 2013

Signature of Author.....
Department of Civil and Environmental Engineering
May 21, 2013

Certified by.....
Herbert H. Einstein
Professor of Civil and Environmental Engineering
Thesis Supervisor

Accepted by.....
Heidi M. Nepf,
Chair, Departmental Committee for Graduate Students

Tunnel Boring Machine (TBM) Performance in Singapore's Mass Rapid Transit (MRT) system

by
Wanling Chong

Submitted to the Department of Civil and Environmental Engineering
on May 21, 2013, in partial fulfillment of the requirements for the degree of
Master of Engineering in Civil and Environmental Engineering

ABSTRACT

Singapore's Mass Rapid Transit (MRT) network is one of the largest public works projects undertaken by the Singapore government. This thesis summarizes and evaluates the performance of Tunnel Boring Machine (TBM) construction in Singapore's MRT network. Surface settlement induced by the tunneling process can cause damage to underground utilities and foundations and buildings and/or disrupt daily life by damaging roads and pavements, and is used in this thesis as a measure of performance. The influence of encountered geology and adopted construction methods (referring to the type of TBM used) on settlement is discussed. The dominant construction method on all four existing MRT lines involved the use of shield TBMs, with the main difference being the method of face support adopted. The North-South East-West (NS-EW) line employed largely compressed air as face support, while a move towards greater use of Earth Pressure Balance (EPB) was observed on the North-East line (NEL) and Circle Line (CCL). The use of EPB on the NEL resulted in 22 incidences of large, localized ground losses, which were of two types; 1. subsurface voids, or voids which formed above the tunnel face but were grouted before they could migrate to the surface, 2. surface sinkholes, or local depressions which were found by visual inspection to appear over the tunnels as the machine advanced. These large, localized ground losses usually occurred when tunneling through different weathering grades within a single formation or through mixed faces of different geological formations. The variability in ground conditions which resulted from these mixed weathering grades and mixed faces is a direct result of extensive tropical weathering of Singapore's soils, and poses a challenge to the performance of EPB machines during construction. The employment of slurry machines on the CCL was intended to mitigate some of the difficulties faced by EPB machines on the NEL, though with limited success. The use of slurry machines on the CCL resulted in the additional problem of slurry discharging to the surface and disrupting traffic. Given Singapore's plans to double the length of her rail network by 2030, the need to understand the impact of construction projects on adjacent structures and surface activities remains just as important, if not more so.

Thesis Supervisor: Herbert H. Einstein
Title: Professor of Civil and Environmental Engineering

ACKNOWLEDGEMENTS

This thesis would not have been possible without Professor Einstein's guidance and advice. I had the good fortune of learning from some of his former students, and it was the greatest honor for me to have learnt from the teacher himself during my past year at MIT. Patient and kind, I am sure I speak for many of his students when I say that his approach to education has left us changed by the experience. He was a source of encouragement and motivation throughout the process, and oftentimes, it felt like his advice was the light at the end of the tunnel guiding me through the process.

The analogy of drinking from a fire hose is often used to describe the learning experience at MIT. If so, then manning the hose must have been these instructors who have generously shared their time, experience and knowledge in teaching me. My heartfelt thanks go out to:
Dr John Germaine, my academic advisor who has taught me much about the intricacies of experimental research;
Dr Lucy Jen, who taught me soil mechanics when I thought I knew it all;
Prof Andrew Whittle, the master of 'cute solutions' and PLAXIS, without whom I might have never dabbled in finite element modeling;
Dr David Langseth, who orchestrated my very first visit to a landfill;
Susan Murcott, who taught me that engineering is not about numbers, but about people too;
and Prof Jerome Connor and Dr Todd Radford: both of whom taught me interesting things about structures though I thought all I had signed up for was geotechnical engineering.

The friends I have made in the M.Eng program are amazing people, and I count it among my blessings that this program has brought us together from different backgrounds to share this experience. To Geotech friends, classes would not have been half as fun without your company. I think I will feel the absence of such like-minded friends in my life most of all when chancing upon an excavation and stopping to observe it no longer becomes socially acceptable behavior. Clichéd as it may sound, my time at MIT truly has been an intensive but meaningful journey of self-discovery.

"We shall not cease from exploration, and the end of all our exploring will be to arrive where we started and know the place for the first time." T.S. Eliot, Four Quartets 4: Little Gidding.

I have never felt so keenly before the absence of my family and friends until I spent this year abroad. Sad as I am to be leaving, my heart is glad to be homeward bound.

TABLE OF CONTENTS

LIST OF FIGURES

LIST OF TABLES

1. INTRODUCTION

1.1 HISTORY OF TUNNELING

For 5000 years, man has tunneled for irrigation, war, mining, transport and various other reasons (Maidl, et al., 1996). Tunneling was a way to go around nature's obstacles, instead of surmounting them. Before modern-day Tunnel Boring Machines (TBMs), tunnel excavation took place by hand-digging or drill-and-blast methods (Bonnett, 2005).

At the start of the 19th century, industrialization and the corresponding push for the construction of a railway network resulted in the rapid development of tunneling (Maidl, et al., 2008). The invention of the shield concept by Marc Isambard Brunel in 1806 opened up the possibility of tunneling in difficult ground conditions, such as under the water table or in unstable ground. The shield acts to temporarily support the tunnel before installation of permanent support/lining, hence minimizing above-ground disturbance (Maidl, et al., 1996). A revolution in tunneling, Brunel's rectangular shield was used to construct the Wapping-Rotherhithe tunnel under the Thames River in 1825 (Lane, 2013); the shield was advanced by hydraulic jacks, and hand excavation was carried out by 36 workers organized in twelve contiguous frames with 3 chambers each (Maidl, et al., 1996). The tunnel took 18 years to complete, with five serious incidences of flooding (Maidl, et al., 1996).

Peter William Barlow and James Henry Greathead improved on Brunel's shield, introducing in 1869 a smaller, circular shield which used cast-iron segments for lining (Lane, 2013; Maidl, et al., 1996). The invention of the airlock by Admiral Sir Cochrane in 1830 (Maidl, et al., 1996), and the successful combined use of a tunneling shield with compressed air by Greathead in 1886 gave rise to compressed air tunneling, which has seen widespread usage in modern times with little change to the original idea (Lane, 2013).

1.2 TUNNEL BORING MACHINES (TBMS)

The move into fully-mechanized excavation has given us the modern-day TBM, although some of the first rock machines actually operated rather differently from today's TBMs (Maidl, et al., 2008). Different people have been credited with inventing the first TBM; Henri-Joseph Maus in 1846, Charles Wilson in 1851 (Maidl, et al., 2008), Beaumont in the early 1880s and James S. Robbins in 1952 (Bieniawski, 1984). Maus' prototype, built in 1846, uses percussive drilling to carve a groove around the tunnel wall, while the rock within the groove is loosened by means of wedges or explosives and removed by hand (Maidl, et al., 2008). Wilson's machine has many elements of modern-day TBMs, and excavates the entire tunnel face using disc cutters (Maidl, et al., 2008). Maus' and Wilson's machines, though sound in principle, did not succeed in actual tunneling; there were doubts about the ability of Maus' machine's drive equipment to deliver sufficient power and cutting force, while Wilson's machine experienced a problem with its disc cutters, and had to be retired after 3m of advance (Maidl, et al., 2008). Beaumont's and Robbins' machines were more successful, with the former achieving a maximum advance rate of 25m a day (Maidl, et al., 2008). Beaumont's two machines, built using Colonel T. English's patent, successfully drove more than 3 km of the Channel Tunnel from 1882 to 1883 (Maidl, et al., 2008) while James Robbins' open gripper TBM with disc cutters was used successfully on the Oahe Dam on the Missouri River, South Dakota (Lane, 2013).

1.2.1 TYPES OF TUNNEL BORING MACHINES

Numerous types of TBMs are now available on the market to optimize tunneling in varied and difficult ground conditions. TBMs are usually differentiated by the degree of support which they provide to the tunnel (Sousa, 2010). A summary of the different types of support provided by TBMs and the suitable ground conditions for use in tunneling is given in Table 1-1.

Most commonly employed TBMs on the construction of Singapore's Mass Rapid Transit (MRT) network were shield TBMs, which can be further differentiated by the methods they use to support at the tunnel face, schematically shown in Figure 1-1. Natural support either relies on the inherent shear strength of the tunnel's geological formation, or on the slope of the excavated material acting against the tunnel face, to maintain face stability (Maidl, et al., 1996). Mechanical support can entail using lagging to support the tunnel face as it is manually excavated from top to bottom, or through the use of hydraulically controlled plates which apply a force/pressure against the tunnel face to maintain stability (Maidl, et al., 1996). Natural and mechanical support cannot, however, prevent the ingress of water when tunneling under the water table (Maidl, et al., 1996).

To counteract water ingress into tunnels, Greathead in 1886 employed the use of a shield with compressed air. Figure 1-2 demonstrates the principle of using compressed air to stabilize the tunnel face: maximum water pressure in the tunnel acts at the invert, and must be counteracted by the applied air pressure in order to prevent water from entering the tunnel (Maidl, et al., 1996). However, in doing that, air pressures at the crown will exceed water pressures, causing air to escape (Maidl, et al., 1996). In coarse-grained soils with high hydraulic conductivities ($k_w > 10^{-4}$ m/s), this escaping air displaces water in voids, and can cause blowouts in cases of insufficient overburden (Maidl, et al., 1996). Successful usage of compressed air during tunneling requires a steady, secure supply of compressed air and sealing of the chambers to ensure airtightness (Suwansawat, 2002). The risk of decompression sickness in workers during tunneling in compressed air also usually calls for the provision of medical support. The use of compressed air counteracts water pressures alone, and earth pressures have to be additionally countered by either natural or mechanical methods (Maidl, et al., 1996).

The use of slurry and Earth Pressure Balance (EPB) were later introduced in order to counter both earth and water pressures (Maidl, et al., 1996). The slurry, a frictionless liquid, is formed through the addition of bentonite to water, the former being frequently employed for its

plasticity and swelling capacity (Maidl, et al., 1996; Suwansawat, 2002). This slurry provies support by forming a filter cake, or a thin, impermeable film, on the tunnel face that transfers pressure (Maidl, et al., 1996; Suwansawat, 2002). EPB is similar in principle, with the major difference being that the excavated soil itself (with addition of conditioning agents) is used in place of slurry to stabilize the tunnel face (Maidl, et al., 1996). The excavated soil is remolded in the earth chamber, forming a plug that supports the tunnel face (Suwansawat, 2002). EPB describes when equilibrium between the earth pressures exerted on the tunnel face and pressures exerted by the remolded soil is attained (Maidl, et al., 1996; Suwansawat, 2002) and is maintained by balancing the volume of material removed by the screw conveyor and volume of material entering the chamber, the latter being dependent on the machine's advance rate (Shirlaw, et al., 2000).

While slurry support and EPB are similar in principle, usage of EPB is more appropriate in soil with high fines content, which has greater ability to form an adequate plug in the earth chamber, while usage of slurry support is more successful in non-cohesive soils (Maidl, et al., 1996; Suwansawat, 2002). The principles of slurry face support and EPB are given in Figures 1-3 and 1-4, respectively.

1.3 History of Tunneling in Singapore

1.3.1 Introduction

The main purpose of tunneling in Singapore to date has been for the construction of transportation infrastructure or installation of utilities, particularly sewer systems. The tunneling industry in Singapore is a relatively young one, with about three decades of history under its belt. A 3km long tunnel constructed in 1983 to contain a sewage pipeline is generally regarded as the earliest tunneling project (Balasubramaniam & Musa, 1993; Hulme & Burchell, 1999). Singapore's Mass Rapid Transit (MRT) network, which currently consists of four lines, and two lines under

construction, is one of the largest public works projects undertaken by the Singapore government. A schematic of Singapore's MRT network is given in Figure 1-5. Major tunneling works in Singapore, given in chronological order, are summarized in Table 1-2.

1.3.2 Mass Rapid Transit (MRT) Network

Tunneling began in 1984 on the first two MRT lines, the North-South (NS) and East-West (EW) lines (Hulme & Burchell, 1992). Given the relative inexperience of local contractors in tunneling tjem, much of the expertise was international. Engineers and contractors came from as near as Malaysia, Thailand and the Philippines, to as far as the United States of America and the United Kingdom (Hulme & Burchell, 1992). The great majority of tunneling methods used in the NS-EW line were Greathead shields with backhoe excavators, in free air and compressed air (Hulme & Burchell, 1992). The relatively short lengths of the drives facilitated the use of these "simple, relatively erected shields", shown in Figure 1-6 (Hulme & Burchell, 1992). For short drives in competent ground, New Austrian Tunneling Method (NATM) was used (Hulme & Burchell, 1992). Two Earth Pressure Balance (EPB) machines were also employed in one contract (Hulme & Burchell, 1992). Figure 1-7 presents the layout of NS-EW line with stations and contract numbers for each drive, while Table 1-3 summarizes the geology and tunneling methods adopted along the NS-EW line. Detailed geological cross-sections of each tunnel drive for the NS-EW line can be found in Appendix A.

While construction on the NS-EW line was mostly complete by 1990, numerous extension projects were carried out in the following years to enhance MRT coverage of the island. The Changi Airport Line (CAL) is one such extension project, and aims to provide affordable public transportation from the city center to Singapore's international airport. Two Lovat Earth Pressure Balance (EPB) machines were employed for the 3.5km drive, which was the longest bored tunnel

drive in Singapore then, to handle possible face instability due to presence of marine clay (Ow, et al., 2004).

Before construction on the first two MRT lines was complete, plans to construct a third line were already in the works (Hulme & Burchell, 1999). The third MRT line, the North-East Line (NEL), began its construction almost immediately as the NS-EW line finished its construction. The NEL differed from the NS-EW line in two main ways: first, the entire 20km of NEL was located underground as opposed to only 16.5% of the NS-EW line; second, majority of the NEL drives utilized EPB machines, with only 2 out of the 24 drives driven with semi-mechanical open shields (Shirlaw, et al., 2001). Figure 1-8 presents geological cross-sections of the tunnel drives along the NEL, while Table 1-4 summarizes the geology and tunneling methods adopted on the NEL.

Construction on the Circle Line (CCL) began as construction on the NEL was nearing completion. Opened to public ridership a decade later, the CCL aims to better connect the various commercial and business districts of Singapore. Similar to the NEL, most of the CCL is located underground, and while majority of the machines employed were EPB machines, a good number of slurry machines were also used in construction (Ow, et al., 2004). Figure 1-9 presents the layout of CCL with stations and contract numbers for each drive, while Table 1-5 summarizes the geology and tunneling methods adopted on CCL.

A fifth MRT line, the Downtown line, is slated to open to public ridership in three stages in the years 2013, 2015 and 2017, while a sixth MRT line, the Thomson line, is currently under construction, and expected to be complete in 2019.

1.3.3 Tunneling Methods Adopted for MRT Construction

Figures 1-10 and 1-11 summarize the relative usage of different construction methods on the four MRT lines. One thing remains common through construction of the different MRT lines: the dominant construction method involved the use of shield TBMs with the main difference being the

method of face support adopted. On the North-South East-West (NS-EW) line, compressed air was largely used as face support, while the North-East line (NEL) saw greater employment of Earth Pressure Balance (EPB), and the Circle Line (CCL) saw both the use of EPB and slurry support. While NEL had a greater proportion of project distance driven by EPB machines, the CCL exceeded the NEL in terms of total distance driven by EPB machines. Being able to eliminate the risk of decompression sickness associated with the use of compressed air (which was the main mode of face support adopted for soft ground in the NS-EW line) by employing EPB instead coincided with improvements in EPB technology (Ow, et al., 2004). This coupled with a growing recognition of tunnel engineers in Singapore of the ability of soft ground to form appropriate spoil material for successful EPB operation, likely resulted in an increased use of EPB machines for the NEL and CCL.

1.4 Motivation and Methodology

This thesis aims to evaluate the performance of TBM construction in Singapore's MRT network through an extensive literature review, using surface settlement as a measure of risk. Surface settlement induced by the tunneling process can cause damage to underground utilities and foundations and buildings, and/or disrupt daily life by damaging roads and pavements (Shirlaw, et al., 2003), and is hence used in this thesis as a measure of performance.

The move to increased usage of EPB machines on the NEL for a wide range of geological conditions resulted in large, localized ground losses due to the inability of the machine to control tunnel face stability. This will be further described in chapter 3, and contrasted with experience on the CCL, which provides an interesting comparison as to how engineers have adopted a variety of solutions to mitigate the occurrence of such large, localized settlements.

Table 1-1: Types of support provided by TBMs (Sousa, 2010; Zhao, 2012)

Type of support	Machine		Suitable ground
None	Reaming machine		Competent rock
	Gripper TBM		Competent rock
Peripheral only	Gripper shield		Firm soil, soft rock
	Segmental shield		Firm soil, soft rock
	Double shield (gripper and segmental)		Firm soil, soft rock
Peripheral and frontal	Mechanical face support shield		Firm soil, weathered and highly fractured rock
	Compressed air shield		Firm soil with groundwater, soil mixed with rock
	Slurry/hydro-shield		Sand, sandy soil (mixed with rock)
	Earth Pressure Balance shield		Clay, clayey soil (mixed with rock)
	Hybrid machines	Mix-Shield	Soil-rock mixed grounds
		Double Shield	Rock-soil changing grounds
		EPB-Slurry Convertible	Clay-sand varying grounds

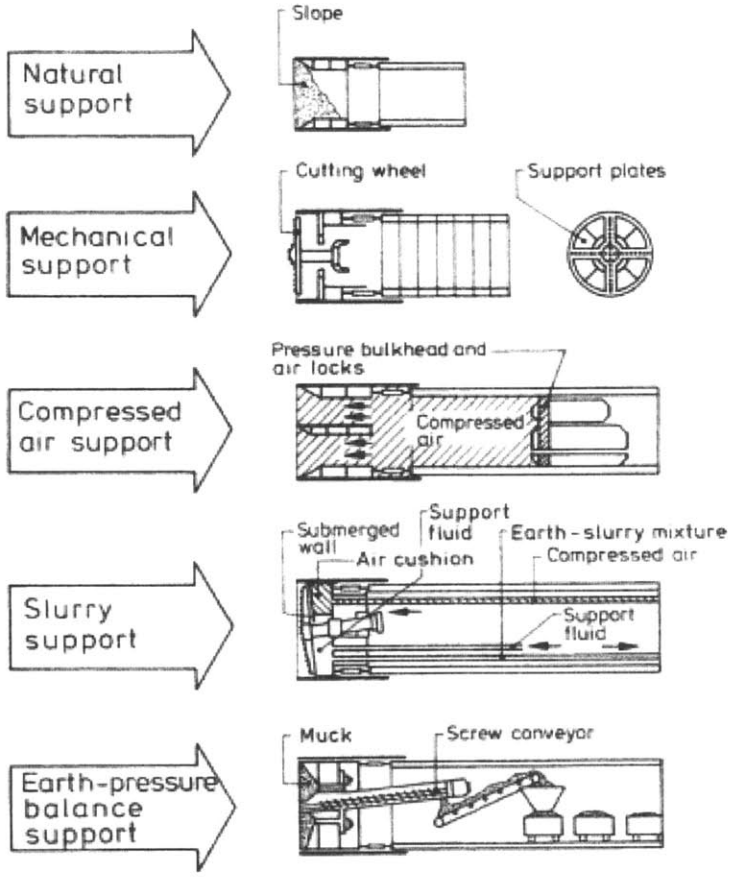

Figure 1-1: Schematic of various face support methods by TBMs (Maidl, et al., 1996)

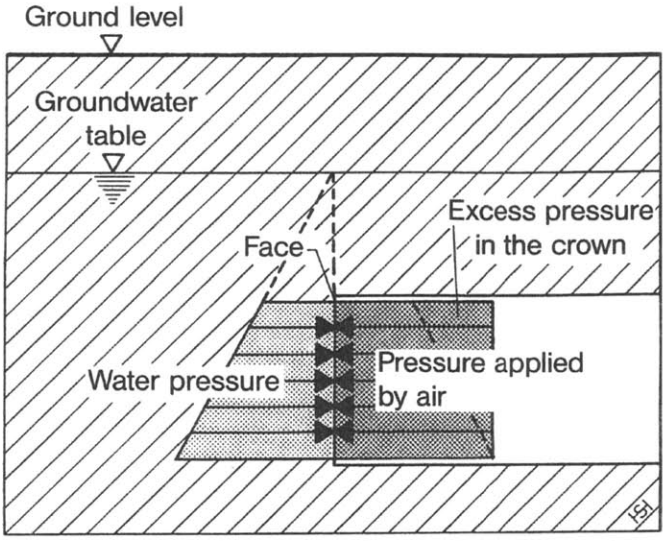

Figure 1-2: Use of compressed air as face support (Maidl, et al., 1996)

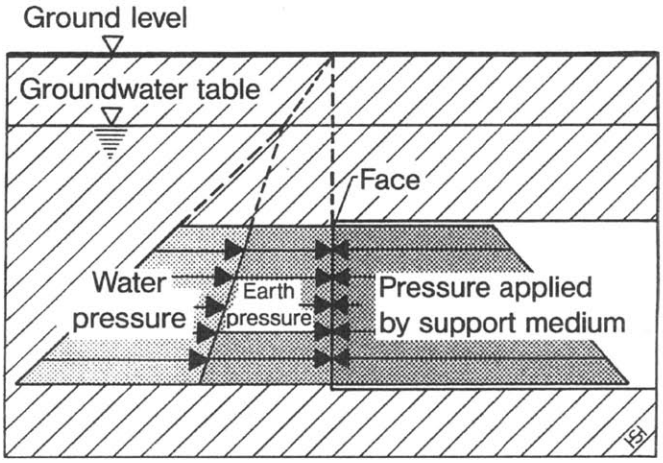

Figure 1-3: Use of slurry as face support (Maidl, et al., 1996)

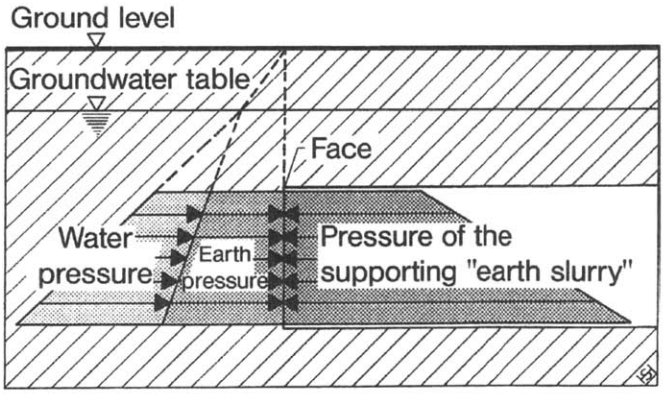

Figure 1-4: Use of earth pressure balance as face support (Maidl, et al., 1996)

Table 1-2: Summary of major tunneling works in Singapore (Balasubramaniam & Musa, 1993; Hulme & Burchell, 1999; Ow, et al., 2004)

Years	MRT Line/ Utility	Total no. of stations	Total length	Above Ground	Belowground	
					Cut and Cover	TBM
1983	Sewage pipeline	-	3.0km	0.0km	0.0km	3.0km
1983-1996	NS-EW	51	66.8km	50.0km	5.8km	11.0km
1999-2002	NS-EW Changi Aiport extension	2	6.0km	2.0km	0.5km	3.5km
1996-2003	NEL	16	20.0km	0.0km	8.5km	11.5km
2002-2012	CCL	31	33.0km	0.0km	4.2km	28.8km
2000-present	DTSS	-	63.4km	0.0km	0.0km	63.4km

TBM: Tunnel Boring Machine; NS: North-South Line; EW: East-West Line; NEL: North-East Line; CCL: Circle Line; DTSS: Deep Tunnel Sewerage Scheme

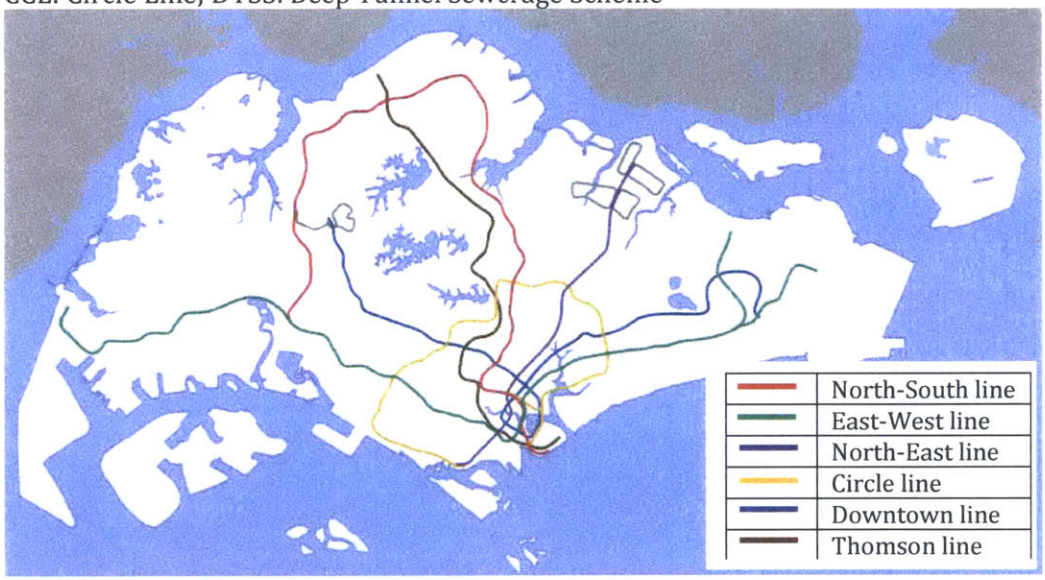

Figure 1-5: Location of Singapore's Mass Rapid Transit (MRT) lines (Wikimedia)

Figure 1-6: Greathead shield employed on NS-EW line, C107B/C301 (Shirlaw & Hulme, 2011, Figure 2)

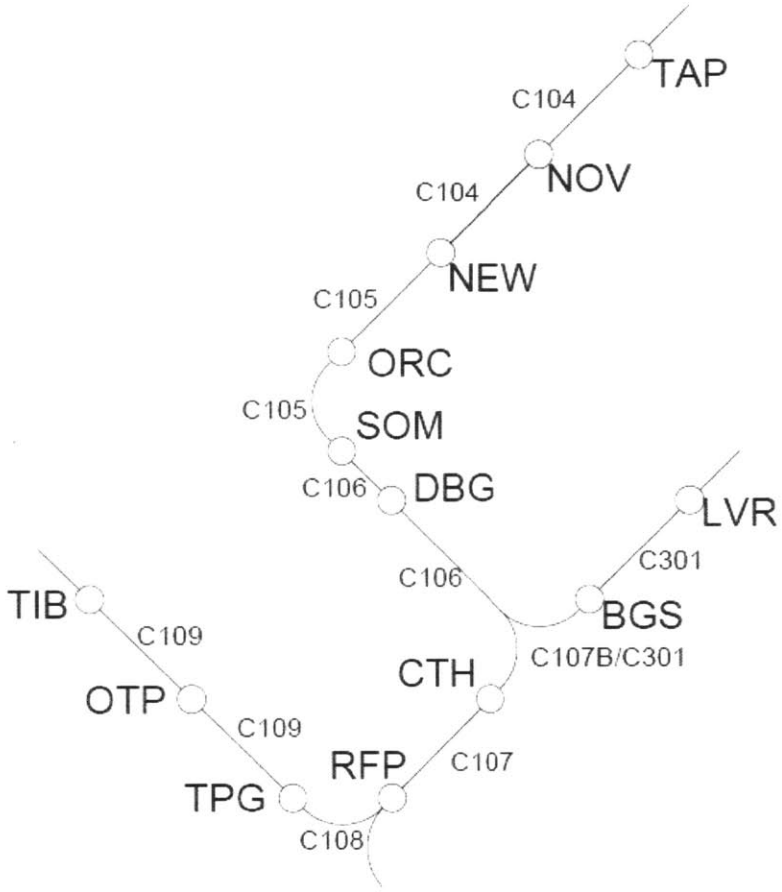

Figure 1-7: Layout of North-South East-West (NS-EW) line

Station name	Abbreviation
Toa Payoh	TAP
Novena	NOV
Newton	NEW
Orchard	ORC
Somerset	SOM
Dhoby Ghaut	DBG
City Hall	CTH
Raffles Place	RFP
Tanjong Pagar	TPG
Outram Park	OTP
Tiong Bahru	TIB
Bugis	BGS
Lavender	LVR

Detailed geological cross-sections for drives along the NS-EW line can be found in Appendix A.

Table 1-3: Summary of tunneling methods and geology along North-South East-West (NS-EW) line (Hulme & Burchell, 1992)

Contract	Drive		Tunneling method	Pressure (bar)	Geology	TBM specifications			
						Manufacturer	Type	Nos.	Ext. Diam. (mm)
C104	TAP	NOV	Shield in CA	0.9-1.6	BTG, KF	Komatsu	Greathead	2	5930
			NATM		BTG, JF				
	NOV	NEW	Shield in CA	0.9	BTG, KF	Hitachi Zosen	Blind	2	5930
C105	ORC	NEW	TBM in CA	1.0	BTG, KF, FCBB	Hitachi Zosen	TBM	1	6410
			TBM in free air		BTG				
	ORC	SOM (SB)	TBM in CA	1.0	BTG, FCBB, KF				
			TBM in free air		BTG, FCBB				
			NATM		BTG				
	ORC	SOM (NB)	Shield in CA	1.0	BTG	Grosvenor	Greathead	1	5850
			Shield in free air		BTG, FCBB, KF				
C106	DBG	SOM	Shield in free air		BTG, JF	Grosvenor	Greathead	2	5850
	DBG	CTH	Shield in free air		JF, FCBB, KF				
			NATM						
C107	RFP	CTH	Shield in CA	CA used when fluvial sand encountered	OA, KF	Keppel-Mitsui	Greathead	3	5970
C107A	RFP	C310	NATM		FCBB				
C107B/ C301	CTH	BGS	Shield in CA	0.9-2.35 (EB), 0.55-1.3 (WB)	FCBB, KF	Nishimatsu-Hiratsuka	Greathead	2	5920
			Shield in free air		FCBB, OA				
C108	TPG	RFP	Shield in CA	1.0-1.8	JF, KF, OA, FCBB	Mitsubishi	Greathead	2	6030
C109	OTP	TPG	Shield in CA	0.5-1.35	JF	Mitsubishi	Greathead	2	5860
	TIB	OTP	Shield in CA	0.5-1.2					
			Shield in free air						
C301	LVR	BGS	EPB		KF	Kawasaki	EPB Shield	2	5930

NATM: New Austrian Tunneling Method; CA: Compressed air; EPB: Earth Pressure Balance; BTG: Bukit Timah Granite; JF: Jurong Formation; FCBB: Fort Canning Boulder Bed; KF: Kallang Formation; OA: Old Alluvium; EB: East-bound drive; WB: West-bound drive

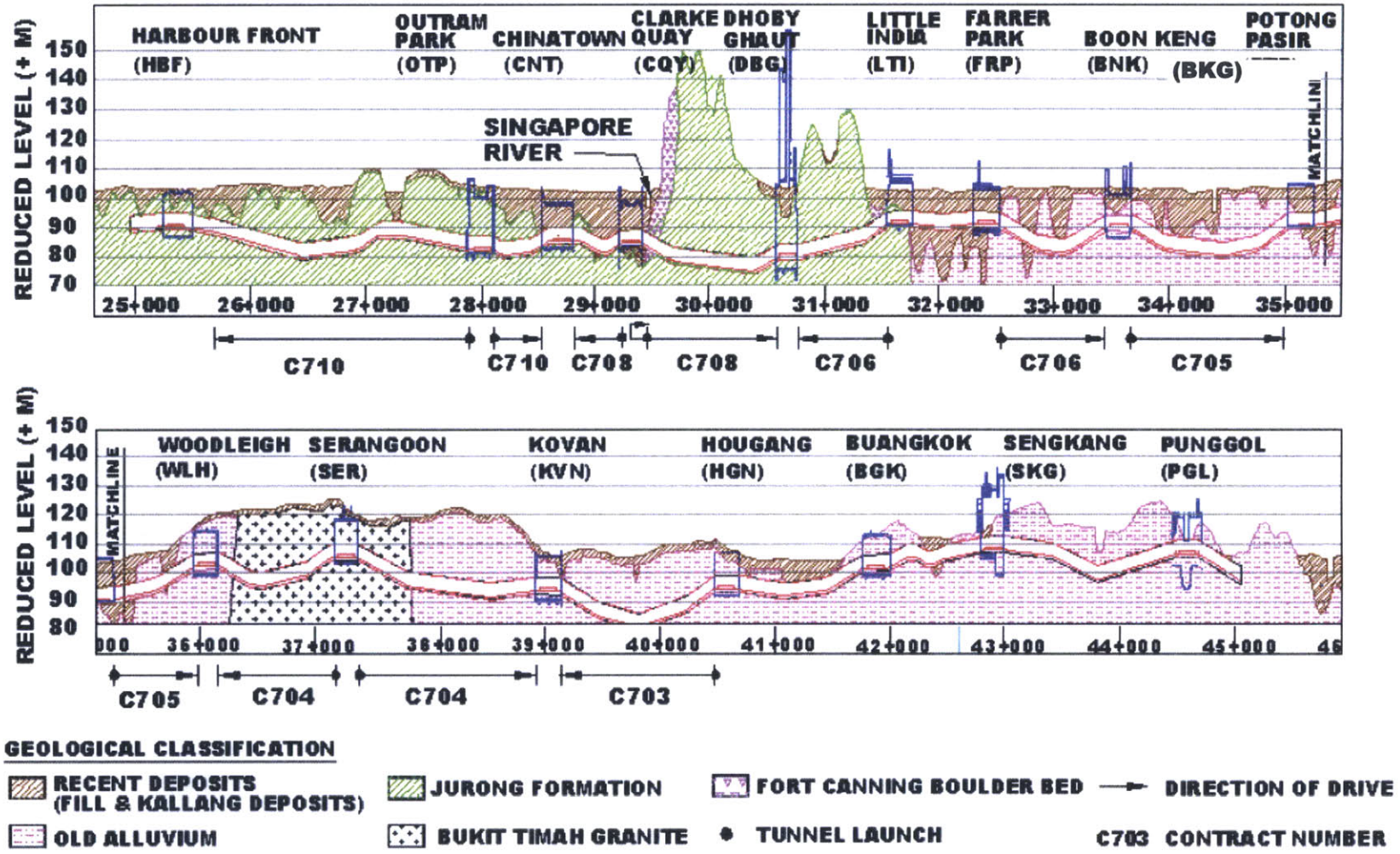

Figure 1-8: Geological cross-section of tunnel drives along the North-East Line (NEL) (Shirlaw, et al., 2001)

Table 1-4: Summary of tunneling methods and geology along North-East Line (NEL) (Hulme & Burchell, 1999; Reilly, 1999)

Contract	Drive		Tunneling method	Geology	TBM specifications			
					Manufacturer	Type	Nos.	Ext. Diam. (mm)
C703	HNG	KVN	EPB	OA	Mitsubishi	EPBM	2	6440
C704	SER	KVN	EPB	OA, BTG	Lovat	EPBM	2	6526
	SER	WLH		BTG, OA				
C705	BKG	PTP	EPB	OA, KF	Hitachi Zosen	EPBM	2	6440
	PTP	WLH						
C706	FRP	BKG	EPB	KF, OA	Herrenknecht	EPBM	2	6550
	LTI	DBG		JF				
C708	CQY	CNT	EPB	KF, JF	Hitachi Zosen	EPBM	2	6480
	River	CQY		FCBB				
	River	DBG	Shield in free air	JF, FCBB	Nishimatsu	OFSM	2	6486
C710	OTP	CNT	EPB	JF, KF	Ishikawa Jima	EPBM	2	6600
	OTP	HBF			Harinaa Heavy Ind	EPBM (dual mode)	2	6600

EPB: Earth Pressure Balance; BTG: Bukit Timah Granite; JF: Jurong Formation; FCBB: Fort Canning Boulder Bed; KF: Kallang Formation; OA: Old Alluvium

Station name	Abbreviation
Hougang	HNG
Kovan	KVN
Serangoon	SER
Woodleigh	WLH
Potong Pasir	PTP
Boon Keng	BKG
Farrer Park	FRP
Little India	LTI
Dhoby Ghaut	DBG
Clarke Quay	CQY
Chinatown	CNT
Outram Park	OTP
Harbourfront	HBF

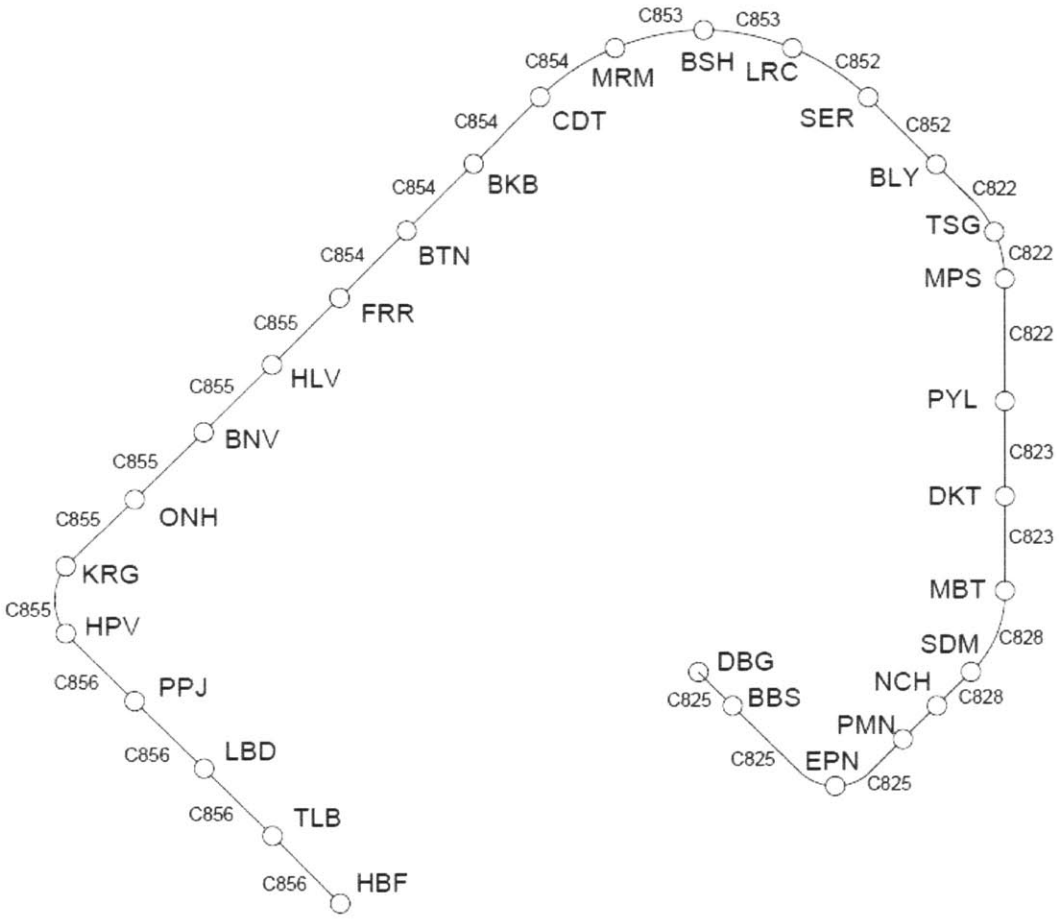

Figure 1-9: Layout of Circle Line (CCL)

Station name	Abbreviation	Station name	Abbreviation
Dhoby Ghaut	DBG	Marymount	MRM
Bras Basah	BBS	Caldecott	CDT
Esplanade	EPN	Bukit Brown	BKB
Promenade	PMN	Botanic Gardens	BTN
Nicoll Highway	NCH	Farrer Road	FRR
Stadium	SDM	Holland Village	HLV
Mountbatten	MBT	Buona Vista	BNV
Dakota	DKT	one-north	ONH
Paya Lebar	PYL	Kent Ridge	KRG
MacPherson	MPS	Haw Par Villa	HPV
Tai Seng	TSG	Pasir Panjang	PPJ
Bartley	BLY	Labrador Park	LBD
Serangoon	SER	Telok Blangah	TLB
Lorong Chuan	LRC	Harbourfront	HBF
Bishan	BSH		

Table 1-5: Summary of tunneling methods and geology along Circle Line (CCL) (Osborne, Knight-Hassell, Tan, & Wong, 2008)

Contract	Drive		Tunneling method	Geology	TBM specifications			
					Manufacturer	Type	Nos.	Ext. Diam. (mm)
C825	PMN	DBG	EPB	OA, JF, FCBB	Herrenknecht	EPBM	2	6580
C828	SDM	NCH	EPB	KF	Hitachi Zosen	EPBM	2	6630
	SDM	MBT						
C823	MBT	DKT	EPB	KF	Hitachi Zosen	EPBM	4	6630
	DKT	PYL						
C822	TSG	BLY	EPB	KF, OA, BTG	Mitsubishi	EPBM	2	6600
	PYL	MPS						
	TSG	MPS						
C852	LRC	SER	EPB	OA, BTG	Herrenknecht	EPBM	2	6630
	SER	BLY						
C853	BSH	LRC	EPB	BTG, OA	Kawasaki	EPBM	2	6680
	MRM	BSH	Slurry	BTG	Kawasaki	Slurry	2	6720
C854	BKB	CDT	Slurry	BTG	Kawasaki	Slurry shield	4	6720
	CDT	MRM						
	BKB	BTN						
	BTN	FRR						
C855	ONH-BNV-HLV-FRR		Slurry	ONH-HLV: JF	Herrenknecht	Mixshield	2	6630
			Slurry	HLV-FRR: BTG				
	ONH-KRG-HPV		EPB	JF	Herrenknecht	EPBM	2	6630
C856	HPV-PPJ-LBD-TLB-HBF		EPB	JF, KF	Herrenknecht	EPBM	3	6600

EPB: Earth Pressure Balance; BTG: Bukit Timah Granite; JF: Jurong Formation; FCBB: Fort Canning Boulder Bed; KF: Kallang Formation; OA: Old Alluvium

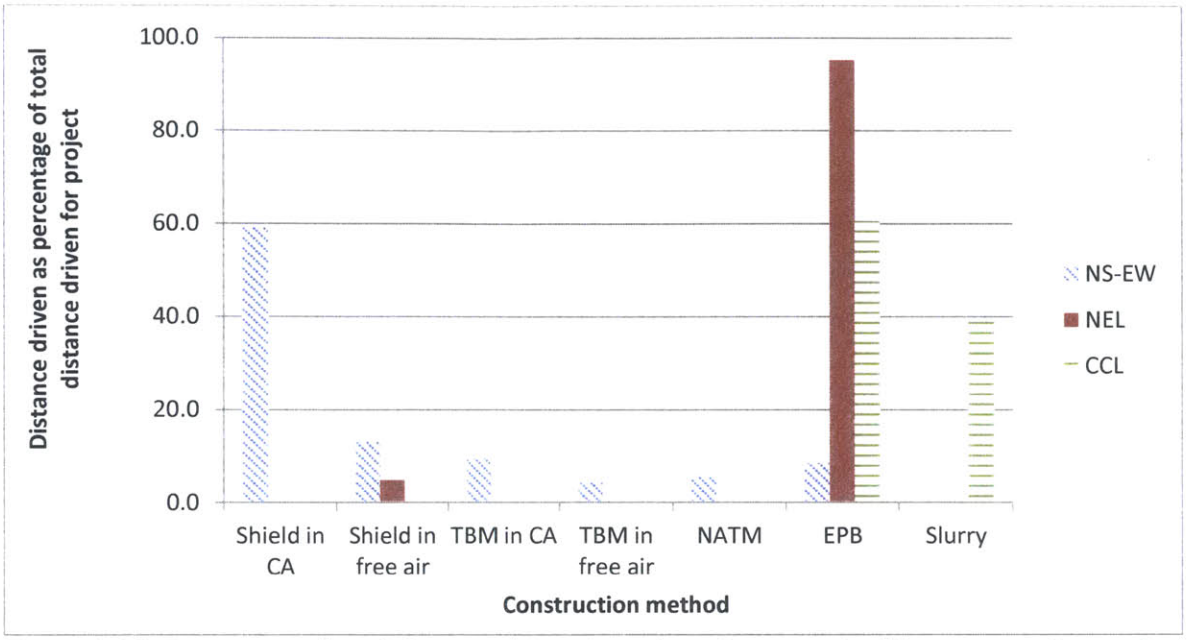

Figure 1-10: Percentage of total distance driven in each project organized by construction method

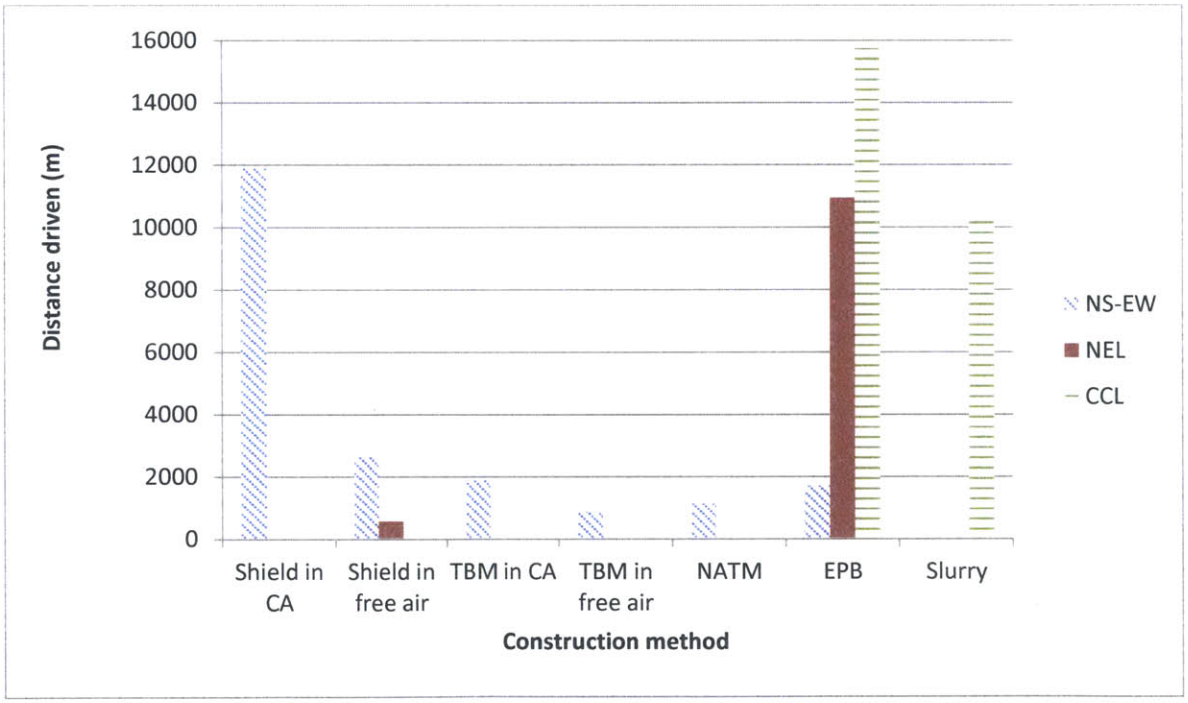

Figure 1-11: Distance driven in each project organized by construction method

2. GEOLOGY OF SINGAPORE

2.1 INTRODUCTION

A simplified map of the major geological formations in Singapore is presented in Figure 2-1. Singapore's geology is closely related to that of West Malaysia (Moores & Fairbridge, 1997). Outcrops of the oldest rock in Singapore (Sajahat Formation and Gombak Norite) are usually found in the Western region (Pitts, 1984). The major underlying geological formations are the Bukit Timah Granite, a granitic material formed by intrusion into existing rock (Pitts, 1984) and the Jurong Formation, largely located in the Western part of Singapore, which is thought to have formed by deposition into a shallow basin created by uplift of Bukit Timah Granite. Consequent tilting, folding and faulting has created a variety of sedimentary rock found as distinct facies of the Jurong Formation (Osborne, et al., 2008). Gupta and Pitts (1992) believe that Singapore's current geology was heavily influenced by alternating processes of erosion and deposition accompanied by fluctuating sea levels in the late Tertiary and Quaternary periods (Moores & Fairbridge, 1997). One of these deposits, the Old Alluvium, is the product of deposition of alluvial sediments (Pitts, 1984). A more recent deposit, the Kallang Formation, consists of sediments with marine, fluvial, littoral, coral reef and estuarine origins (Pitts, 1984). Table 2-1 summarizes the major geological formations and their constituent materials in chronological order of formation.

2.2 TROPICAL WEATHERING OF FORMATIONS IN SINGAPORE

Singapore's climate is characterized by high temperatures and abundant rainfall, a result of its close proximity to the equator. Average rainfall data from the Meteorological Service of Singapore are presented in Figure 2-2 (LTA, 2010). These meteorological conditions intensify the weathering process with the implication that it is possible to encounter completely weathered rock up to great depths (Pitts, 1984). In accordance to BS 5930: 1999 "Code of practice for site

investigations", Singapore adopts Approach 2: Classification for Uniform Materials, and uses six grades (Grades I to VI) to describe the degree of weathering in rock formations (BSI, 1999). Figures 2-3 and 2-4 contain the weathering classifications adapted from BS5930: 1999 for the Bukit Timah Granite and the Jurong Formation, respectively (LTA, 2010).

2.2.1 Bukit Timah Granite

The Bukit Timah Granite is an igneous formation consisting of granodiorite, ademellite and granite (Pitts, 1984). Most of what we know about Bukit Timah Granite has been encountered mainly in two areas, Mandai and Serangoon, of which their locations are marked in Figure 2-1 (Shirlaw, et al., 2000). Much of the weathered Bukit Timah Granite encountered in Mandai is residual soil (Grade VI), with small depths of completed weathered rock (Grade V) encountered (Shirlaw, et al., 2000). Transitions from completed weathered rock (Grade V) to fresh or slightly weathered rock (Grades I and II) are sudden (Shirlaw, et al., 2000). This is unlike the classic strong rock weathering profile one would expect, with more gradual transitions between fresh and weathered rock and the presence of core boulders, and observes in the weathering profile in Serangoon (Shirlaw, et al., 2000).

One explanation for the difference in weathering profiles in Mandai and Serangoon could be the difference in hydraulic conductivities of the Bukit Timah Granite in these two areas (Shirlaw, et al., 2000). The Bukit Timah Granite in Mandai has very low hydraulic conductivities in the order of magnitude of 10^{-9} m/s, 2 to 3 orders of magnitude less than that found of the Bukit Timah Granite in the Serangoon area (Shirlaw, et al., 2000. A higher hydraulic conductivity produces greater intrusion of water into the rock mass, which facilitates the weathering process, and could explain why more gradual transitions between weathering grades can be found in the Serangoon area. Engineering properties of different weathered grades of the Bukit Timah Granite can be found in Table 2-2 (Sharma, et al., 1999).

2.2.2 JURONG FORMATION

The Jurong Formation is a sedimentary formation that contains beds of conglomerate, sandstone, siltstone, mudstone and limestone (Moores & Fairbridge, 1997; Pitts, 1984). Extensive folding and faulting is present, even at depths in fresh rock, with some degree of metamorphism (Pitts, 1984; Shirlaw, et al., 2000). The effect of Singapore's tropical climate on the extent of weathering observed in the Jurong Formation rocks is particularly intensive (Sharma, et al., 1999). Table 2-3 summarizes the engineering properties of different rocks found in Jurong Formation (Sharma, et al., 1999), and it can be seen that even within the same formation, the strength of the component rocks varies widely. This, compounded with weathering, results in divergent rock strengths (Sharma, et al., 1999). Values of point load strength indexes for different rocks weathered to different extents are presented in Table 2-3, and are used as a first estimate of rock strength (Sharma, et al., 1999). Strong to very strong range of rocks tend to be slightly weathered conglomerates, sandstones and siltstones, as contrasted to very weak to weak rocks which would be the highly to moderately weathered slates and phyllites (Sharma, et al., 1999). Weathering penetrates down beds of rock instead of down individual joints (as in the case of Bukit Timah Granite), and it is thus rare to encounter core boulders in weathered Jurong Formation (Shirlaw, et al., 2000).

Residual soil of the Jurong Formation can be described as a stiff to hard, cohesive material, which due to the variability of its parent rock and frequent presence of faulting, has inherited the same heterogeneity that is associated with Jurong Formation rocks as described above (Sharma, et al., 1999). This heterogeneity manifests itself as interbedded layers of clayey silt, sandy clay and clayey to silty sand (Sharma, et al., 1999). Engineering properties of residual soil of Jurong Formation are given in Table 2-4.

Although considered by many to be a facies of the Jurong Formation, the Fort Canning Boulder Bed consists of sandstone boulders in a clayey, sandy silt matrix (Pitts, 1984), and as such

is more analogous to weathered igneous rock with core boulders than weathered Jurong Foundation (Shirlaw, et al., 2000).

2.2.3 Old Alluvium

The Old Alluvium consists of alluvial deposits of medium dense to very dense clayey coarse sand, fine gravel and lenses of silt and clay (Pitts, 1984). It is presumed that the source of these deposits was mechanical erosion of granite from Indonesian and Malaysian mountains (Shirlaw, et al., 2000). Burton (1964) devised three weathering grades for Old Alluvium: weathered zone, mottled zone and unweathered or intact zone (Sharma, et al., 1999). In the weathered zone, there is almost complete destruction of ferro-magnesian minerals, complete alteration of feldspars to kaolin and dissolution of some quartz (Sharma, et al., 1999). This weathering classification has been improved on by Li (1999) by including blow counts from Standard Penetration Tests as a more quantitative way to describe weathering (Sharma, et al., 1999). Engineering properties of Old Alluvium are summarized in Table 2-5 (Sharma, et al., 1999).

2.3 Engineering Considerations

Singapore's geology poses engineering challenges due to the variation of geological formations found, and extensive tropical weathering. Some implications for tunneling are explored.

2.3.1 Variation in Geology along Tunnel Drive

Figure 2-5 presents a plan view of Singapore's MRT network and the geological formations encountered along the tunnel drives. Machine selection and operation had to account for these geological variations, which were not only due to changes in geological formation, but also due to changes in soil properties given different extents of weathering (Hulme & Burchell, 1992).

2.3.2 Possibility of Mixed Face Conditions

A mixed face condition, which comprises encountering a strong material (e.g. rock) and a much weaker material (e.g. soil) in the tunnel face, poses challenges to tunneling (Shirlaw, et al., 2000). Extensive tropical weathering of rocks in Singapore increases the possibility of encountering mixed faces within a tunnel drive for two reasons, the first being that weathering results in a wide variation in material properties within a formation. Grades I to III Bukit Timah Granite behave as rock, as opposed to Grades IV and V, which become flowing ground when exposed below the water table in the tunnel face, while Grade VI residual soil due to its low hydraulic conductivity and high clay content is a reasonable tunneling medium (Shirlaw, et al., 2000). The possibility of encountering mixed face conditions increases when numerous weathering grades are present within a formation, especially at shallow depths where weathering is more extensive than at greater depths. Tropical weathering, which may proceed unevenly depending on the presence of joints, or some other preferential pathway for water to infiltrate, also has the potential to create valleys which are subsequently infilled by weaker material (Shirlaw, et al., 2000). The creation of such valleys increases the possibility that a tunnel drive will pass through these mixed face conditions. The geological cross-section of the tunnel drives for the North-East Line (NEL), as shown in Figure 1-8, shows numerous valleys in the Jurong Formation infilled with marine clay of the Kallang Formation (Shirlaw, et al., 2000).

2.3.3 Presence of Marine Clay in Kallang Formation

While the Kallang Formation consists of deposits with marine, fluvial, littoral, coral reef and estuarine origins, the presence of marine clay dominates the geotechnical performance of this formation. Consisting mostly of kaolinite with a flocculated structure (Sharma, et al., 1999), the natural water content of the marine clay is close to the liquid limit. This, combined with low

cohesive strength, results in the potential for large settlements (Pitts, 1984). Engineering properties of the marine clay are summarized in Table 2-6.

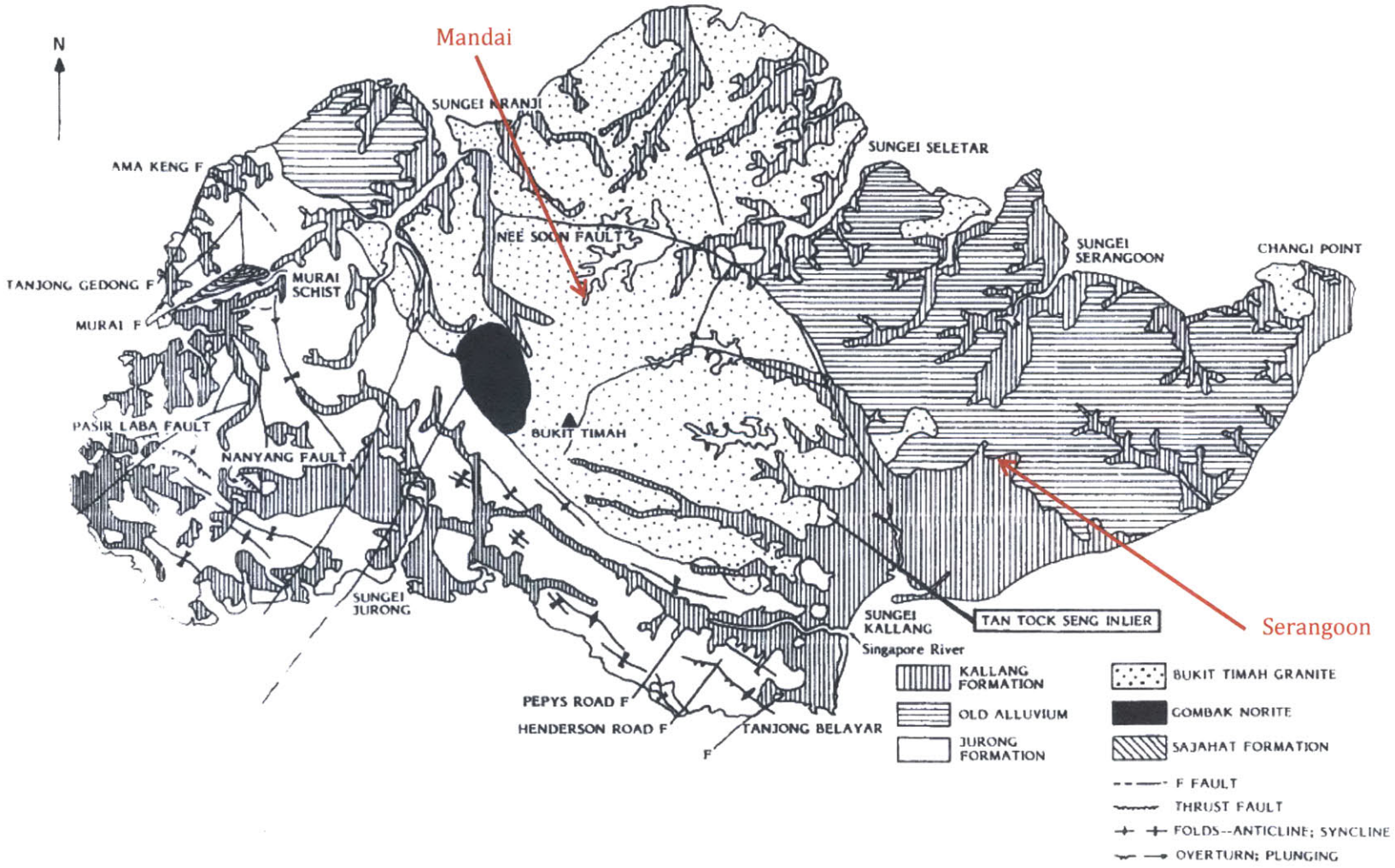

Figure 2-1: Simplified geological map of Singapore (Pitts, 1984, Figure 1)

Table 2-1: Summary of major geological formations in Singapore

	Age	Name/Notation	Formation	Material
Pre-Pleistocene formations	Early Paleozoic	Sajahat Formation	Similar to Pahang Volcanic Series in West Malaysia	Quartzite, sandstone, mudrock, interbedded tuff
	Late Paleozoic	Gombak Norite	Intrusion into pre-Paleozoic rock	Noritic gabbro, gabbro
	Early to middle Triassic	Bukit Timah Granite	Plutonic origin, formed by intrusion into pre-Paleozoic rock	Granodiorite, ademellite, granite
	Late Triassic to middle Jurassic	Jurong Formation	Deposition in shallow basin created by uplift of granite Variability created by tilting, folding and faulting processes	Exists as numerous facies which comprise conglomerate, sandstone, siltstone, mudstone and limestone
Quaternary deposits	Upper Triassic to middle Jurassic	Fort Canning Boulder Bed	Proposed by Pitts (1984) as a Jurong Formation facies, possibly formed by rocks sliding onto clay	Sandstone boulders in a stiff to hard clayey, sandy silt matrix
	Early Pleistocene	Old Alluvium	Deposition of alluvial sediments in basin/trough	Medium dense to very dense clayey coarse sand, fine gravel, lenses of silt and clay
	Late Pleistocene to Recent	Kallang Formation	Deposition of sediments with marine, fluvial, littoral, coral reef and estuarine origins	Marine clay: kaolinite-rich

Summarized from DSTA (2009), Moores & Fairbridge (1997) and Pitts (1984).

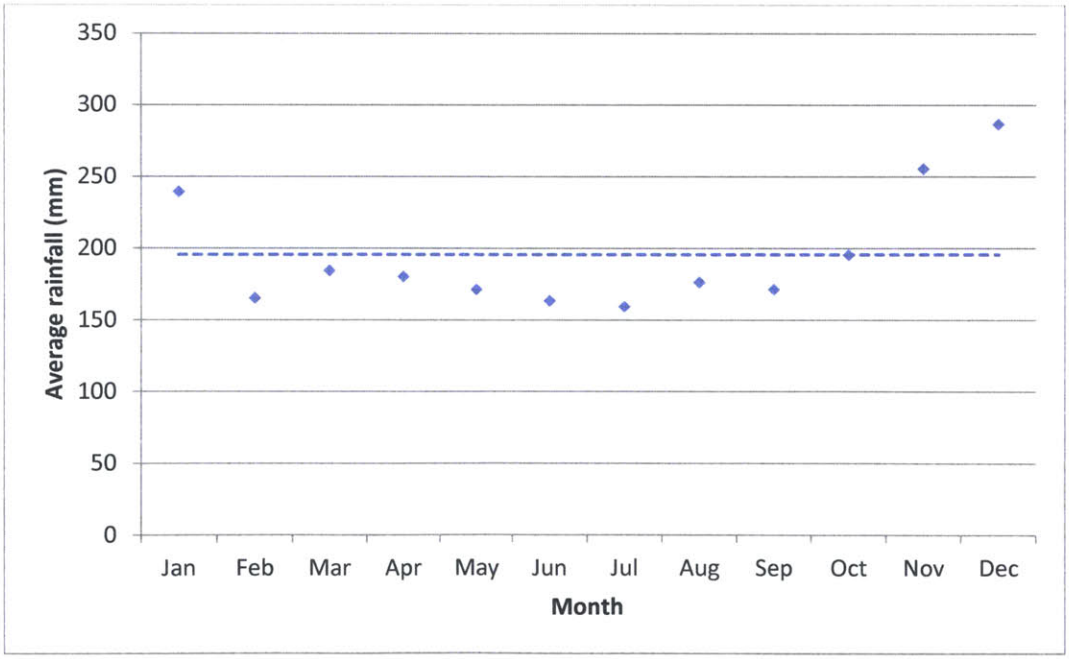

Figure 2-2: Average rainfall data from 1869 - 2003 (135 years) from Meteorological Service of Singapore (LTA, 2010)

Weathering Classification for Bukit Timah Granite & Gombak Norite

in accordance with Approach 2 in BS Code 5930 Section 6 (1999)

Geo-Notation	Grade / Class	Classification	Basis for assessment
G(1)	I	fresh	intact strength unaffected by weathering; not broken easily by hammer; rings when stuck with hammer; no visible discoloration.
G(II)	II	slightly weathered	not broken easily by hammer; rings when stuck with hammer; fresh rock colors generally retained but stained near joint surfaces.
G(III)	III	moderately weathered	**cannot be broken by hand** but easily broken by hammer; makes a dull or slight ringing sound when stuck with hammer; stained throughout.
G(IV)	IV	highly weathered	core can be **broken by hand**; **does not slake in water**; completely discoloured.
G(V)	V	completely weathered	original rock texture preserved; can be crumbled by hand; **slakes in water**; completely discoloured.
G(VI)	VI	residual soil	original rock structure completely degraded to a soil with none of the original fabric remains; can be crumbled by hand

Figure 2-3: Weathering classification for Bukit Timah Granite (LTA, 2010)

Weathering Classification for Jurong Formation

in accordance with Approach 2 in BS Code 5930 Section 6 (1999)

Geo-Notation	Grade / Class	Classification	Basis for assessment
S(I)	I	fresh	intact strength unaffected by weathering
S(II)	II	slightly Weathered	slightly weakened with slight discoloration particularly along joints
S(III)	III	moderately weathered	considerably weakened & discolored; larger pieces **cannot be broken by hand** (RQD generally > 0 but RQD should not be used as the major criterion for assessment)
S(IV)	IV	highly weathered	core **can be broken by hand**; generally highly to very highly fractured but majority of sample consists of lithorelics (RQD generally is 0 but RQD should not be used as the major guide for assessment). For siltstone, shale, sandstone, quartzite, and conglomerate, the **slake test** can be used to differentiate between Grade V (slake) and Grade IV (does not slake)
S(V)	V	completely weathered	rock weathered down to soil-like material but bedding still intact; material **slakes in water**.
S(VI)	VI	residual soil	rock degraded to a soil in which none of the original bedding remains.

Figure 2-4: Weathering classification for Jurong Formation (LTA, 2010)

Table 2-2: Engineering properties of different weathered grades of Bukit Timah Granite (Sharma, et al., 1999)

Weathering grade		ρ_{bulk} (g/cm^3)	**SPT** N-value	**RQD** (%)	$I_{s(50)}$ (MPa)	σ_c (MPa)	v_p (km/s)	E_d (GPa)	**k (x 10^{-9})** (m/s)
Residual soil	VI	2.09	13				1.2	4.5	1.0*
Completely weathered	V	2.14	33				0.9	5.4	
Highly weathered	IV	2.32	>100	45	1.8	32	0.7	5.4	5.12
Moderately weathered	III	2.43		83	5.6	88	4.8	33.2	1.8
Slightly weathered	III	2.54		96	9.9	165	5.6	56.2	1.59
Fresh granite	I	2.66		99	11.1	192	5.8	60.3	0.58

ρ_{bulk}: bulk density; SPT: Standard Penetration Test; RQD: Rock Quality Designation; $I_{s(50)}$: Point load strength index; σ_c: uniaxial compressive strength; v_p: velocity of compression wave; E_d: dynamic modulus of elasticity; k: hydraulic conductivity of rock mass
*Normally consolidated range

Table 2-3: Engineering properties of different rocks in Jurong Formation (Sharma, et al., 1999)

Rock type	**Weathering grade**	$I_{s(50)}$ (MPa)	σ_c (MPa)		E_{ave} (GPa)	$\sigma_{t,avg}$ (MPa)	v_p (km/s)
			Range	Ave			
Conglomerate	Slightly weathered to fresh	3-12	32-102	52	33	9.5	1.2-3
Sandstone	Highly to moderately weathered	0.1-3	35-137	68	57	12.4	1.25-3
Siltstone			21-53	34	38	7.2	1.25-2
Slaty shale/ phyllite	Slightly weathered to fresh	0.3-6	41	41	39	-	1.25-2
	Highly to moderately weathered	<0.1-0.3					
Limestone/ marble	Slightly weathered to fresh	3-12	45-162	88	98	13.4	2-4.5
	Highly to moderately weathered	0.1-3					

$I_{s(50)}$: Point load strength index; σ_c: uniaxial compressive strength; v_p: velocity of compression wave; E_{ave}: average modulus of elasticity; $\sigma_{t,avg}$: average Brazilian tensile strength; k: hydraulic conductivity of rock mass

Table 2-4: Engineering properties of Jurong Formation residual soil (Sharma, et al., 1999)

Engineering properties	**Values**
Natural water content (w), in %	15-45
ρ_{bulk} in g/cm3	1.8-2.2
Specific gravity (G_s)	2.6-2.75
Liquid limit (W_L), in %	28-60
Plastic limit (W_P), in %	14-36
Hydraulic conductivity (k), in m/s	10^{-5} to 10^{-9}
Compression index (C_c)	0.1-0.6
Cohesion (c'), in KPa	0-40
Angle of internal friction (ϕ'), in degrees	24-40

Table 2-5: Engineering properties of different weathering grades of Old Alluvium (Sharma, et al., 1999)

Zone	**Approx depth** (m)	**SPT** N-value	**Description**		
			Color	Composition	Consistency
OA1	0.6-8.0	≤25	Yellowish, reddish or grayish brown	Clayey and silty sand, clayey silt	Loose to medium dense (sands); medium stiff to very stiff (clays)
OA2	8.0-13.0	26-100	Yellowish brown to light gray or greenish gray	Clayey and silty sand	Medium dense to very dense (sands); very stiff to hard (clays)
OA3	>13.0	>100	Light gray to greenish gray	Clayey and silty sand	Very dense to moderately strong

Table 2-6: Engineering properties of marine clay in the Kallang Formation (Sharma, et al., 1999)

	Liquid Limit, %	Plastic Limit, %	Natural water content, %	Undrained shear strength, s_u, kPa
Upper member	70-90	25-30	65-90	10-30
Lower member	70-85	25-30	50-65	30-60
	Over-consolidation ratio, OCR	Compression index, Cc	Recompression index, Cr	Coeff of consolidation, c_v, m^2/yr
Upper member	1.5-2.0	0.6-1.5	0.08-0.16	0.5-1.0
Lower member		0.6-1.0	0.14-0.2	0.8-1.5

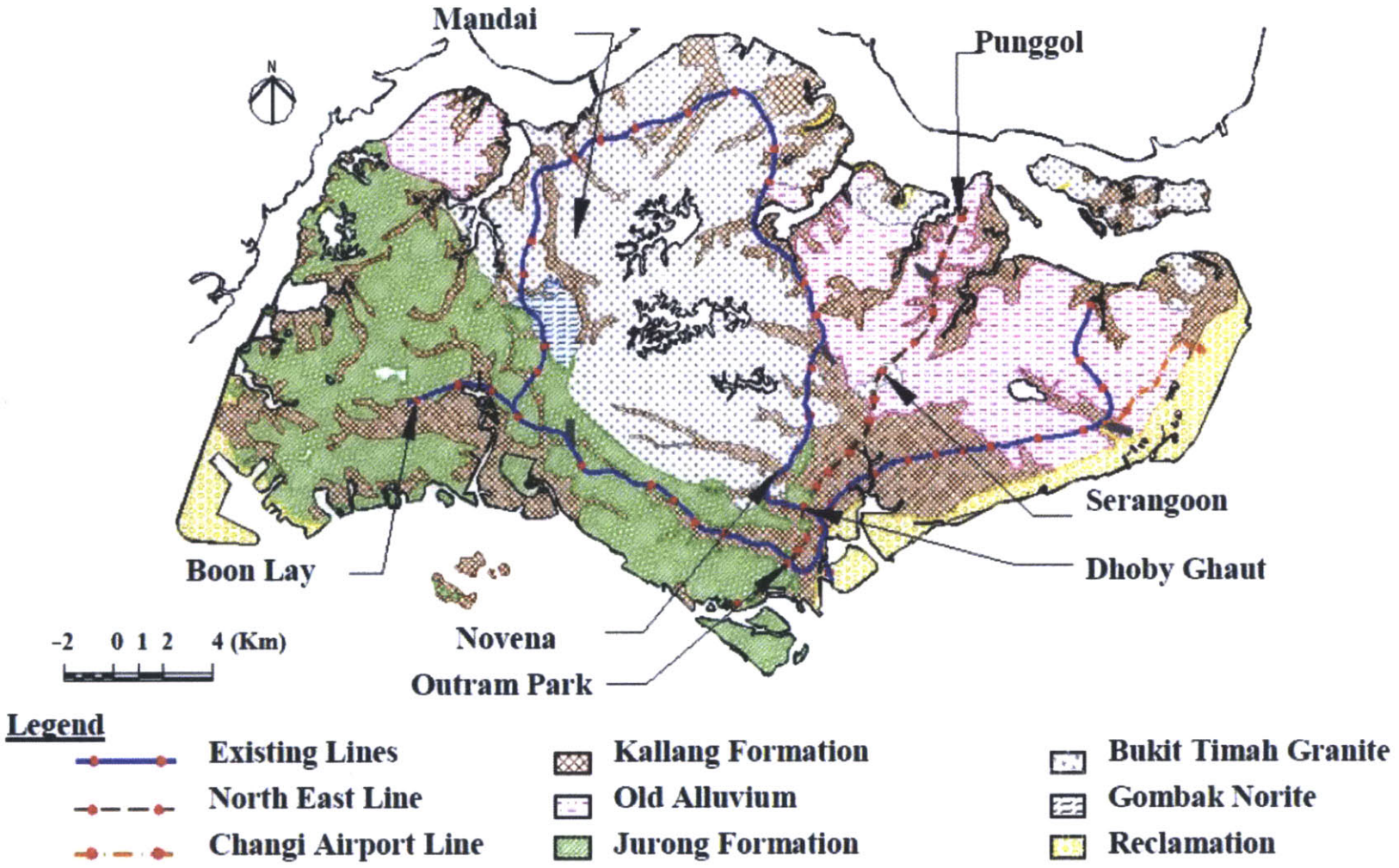

Figure 2-5: Geological formations along Singapore's MRT network (Shirlaw, et al., 2003)

3. SETTLEMENT DUE TO TBM CONSTRUCTION OF SINGAPORE'S MRT NETWORK

3.1 SETTLEMENT OVER TUNNELS

One important measure of Tunnel Boring Machine (TBM) construction performance is the settlement it induces over tunnels, which has the potential to affect surface activities and structures or buried utilities (Shirlaw, et al., 2003). Major tunneling projects often install arrays of ground settlement markers over tunnels to measure settlement during and after construction. Immediate settlement, or settlement observed during construction, depends on the stability of the tunnel face as the machine is launched, advanced or docked, and/or the speed with which the tail void is grouted as the shield passes, amongst other factors (Shirlaw, et al., 2005; Shirlaw, et al., 2001). Long-term settlement, or settlement which can occur months after construction, is usually due to consolidation settlement, which arises from groundwater seepage towards the tunnel, or dissipation of excess pore pressures generated by tunneling (Shirlaw, et al., 2001).

3.2 SETTLEMENT MEASURED FOR THE NORTH-SOUTH EAST-WEST (NS-EW) LINE

Surface settlement values encountered during tunneling for the North-South East-West (NS-EW) line are summarized in Table 3-1 (Hulme & Burchell, 1992). The values in Table 3-1 have been presented as plots in Figures 3-1, 3-2 and 3-3. From Figure 3-1, which organizes settlement by tunnel drive, it can be seen that even within a single drive, numerous construction methods were employed to better control settlements in the different geological formations. For example, for Contract 104, as the tunnel was driven from Toa Payoh (TAP) to Novena (NOV), Greathead shields with both compressed and free air were used, and three geological formations were encountered.

3.2.1 Influence of Geology on Settlement

Organizing the settlement values by geological formation, then construction methods, as presented in Figures 3-2 and 3-3, allows us to analyze the settlements in greater detail.

Bukit Timah Granite: From Figure 3-2, in general, settlements in the Bukit Timah Granite were well-controlled when tunneled with Greathead shields in both compressed and free air and the New Austrian Tunneling Method (NATM), with maximum settlements of 100mm obtained. Large settlements were obtained in two cases where tunnel boring machines (TBMs) were used. Usage of the TBM in free air resulted in high settlement values of 300mm because the volume of soil removed compared with the forward advance of the machine was not effectively controlled (Hulme & Burchell, 1992), resulting in over-excavation. Application of compressed air with TBM usage afforded only slightly better control, and maximum settlement on that drive was 120mm (Hulme & Burchell, 1992).

Jurong Formation: Settlements in the Jurong Formation were generally well-controlled with the use of Greathead shields in compressed air or NATM, and settlements were kept within the range from 5mm to 100mm. However, extremely large settlements were encountered with the use of Greathead shields driven in free air, due to the presence of completely weathered Jurong Formation in one case, and faulted zones in the other, in the tunnel face (Hulme & Burchell, 1992). Without face support, large settlements of 350mm and 200mm, respectively, occurred under these "friable, raveling conditions" (Hulme & Burchell, 1992).

Kallang Formation: For the Kallang Formation, minimum settlement values are in the range of 20mm to 30mm, larger than that for the Bukit Timah Granite and the Jurong Formation, which are in the range of 5mm to 10mm. Settlements in the Kallang Formation were generally better controlled with shields in compressed air than shields in free air, although at times in order to control face stability, air pressures as high as full hydrostatic pressures had to be applied (Hulme & Burchell, 1992). An example in which insufficient face pressures applied resulted in increased

settlement occurred on drive 15 (C104 TAP-NOV), indicated in Figure 3-2; as the tunnel was driven under a canal, employed air pressures were decreased to minimize blow-out risk, resulting in an increased maximum settlement of 100mm from values as low as 30mm to 50mm (Hulme & Burchell, 1992). Extremely large settlements from 200mm to 400mm were encountered when a TBM was used, even in compressed air, because, similar to the case for the Bukit Timah Granite, there was no effective control of the volume of soil removed as the machine advanced (Hulme & Burchell, 1992). Earth pressure balance (EPB) machines exerted good control of initial settlements, which were about 30mm, though consolidation settlements which resulted from the use of EPB resulted in final settlement values that were about four times larger (Hulme & Burchell, 1992).

Old Alluvium: Tunneling in the Old Alluvium using Greathead shields with compressed air resulted in well-controlled settlement of about 20mm.

3.2.2 Influence of Construction Methods on Settlement

It is also useful to consider settlements from the perspective of construction methods employed by referring to Figure 3-3, since these methods are generally chosen with some intention to control settlement for the relevant geological formations they are to be employed in.

Greathead shields: It would be expected that the usage of a shield in compressed air would provide better control of settlement, as opposed to the usage of a shield in free air, due to the better face stability afforded by the compressed air. This is observed to a greater extent for the Jurong Formation and the Kallang Formation, as opposed to that observed for the Bukit Timah Granite. For the Bukit Timah Granite, the use of compressed air with shields accorded only slightly better settlement control than shields with free air, reducing maximum settlement values from 60mm to 40mm. The use of compressed air during shield tunneling was much more effective in reducing maximum settlements for the Kallang Formation, which were half that of settlements obtained during free air shield tunneling. Settlement control with the use of compressed air in the Jurong

Formation was very effective as seen from the large differences in settlements observed in when shields were used in free air as opposed to compressed air, where maximum settlement values were reduced from 350mm to 100mm, and this was because friable, raveling rock was encountered in the tunnel face during free air shield tunneling.

TBMs: The use of TBMs in the Bukit Timah Granite and the Kallang Formation resulted in large settlements due to uncontrolled over-excavation during tunneling. The use of compressed air with the TBM in the Bukit Timah Granite was significant in reducing settlements, though in the Kallang Formation, excessive settlements were observed even with the use of compressed air.

NATM: Use of the NATM in both the Bukit Timah Granite and the Jurong Formation effectively controlled settlements, which were in the range of 10mm to 100mm, possibly because NATM was utilized only when the ground was judged to be competent, and short tunneling lengths were involved, which skews the results (Hulme & Burchell, 1992).

EPB: It was found that while initial settlements from usage of EPB machines were good, it had the undesirable consequence of inducing much larger consolidation settlements (Hulme & Burchell, 1992). Nevertheless, in the presence of the Kallang Formation, EPB seems to provide the best settlement control after tunneling shields in compressed air, the latter of which poses risks to human health which cannot be discounted.

3.3 Settlement Measured for the North-East Line (NEL)

3.3.1 Settlement Monitoring Program

Ground settlement markers were installed at intervals from 15m to 50m along the tunnel axis, while lateral arrays were installed at intervals of about 200m (Shirlaw, et al., 2001). 617 monitoring points which were located laterally within 3m from the tunnel centerline were analyzed (Shirlaw, et al., 2001). Using settlement data from those points, Shirlaw, et al. (2001) calculated

relative volume loss due to tunneling, which is an expression of the area of the settlement trough as a proportion of tunnel area, and is given by the equation below:

$$V_l = \frac{2.5 \cdot i \cdot S_{max}}{A}$$

where V_l is relative volume loss, i is distance from the tunnel centerline to the point of inflection, S_{max} is assessed immediate settlement and A is cross-sectional area of tunnel (Shirlaw, et al., 2001). An example of surface and subsurface settlement profiles over tunnels is given in Figure 3-4 (Mair, Taylor, & Bracegirdle, 1993).

The distance from the tunnel centerline to the point of inflection, i, is normally given as:

$$i = K \cdot z_o$$

where $K$is a settlement trough width parameter and z_o is the depth to the tunnel axis (Shirlaw, et al., 2001). Typical values of Kas recommended by Singapore's Land Transport Authority (LTA) are presented in Table 3-2 (LTA, 2010), while the Kvalues adopted in the analysis by Shirlaw, et al. (2001) are presented in Table 3-3.

Design-and-build contractors and designers in their prediction of settlement over tunnels, regard relative volume loss of 1% to 2% as the conservative upper limit for most formations, with the exception of Kallang Formation (Shirlaw, et al., 2003). Due to the presence of marine clay in Kallang Formation, greater settlements are expected, and a relative volume loss of 2% to 3% is a better benchmark (Shirlaw, et al., 2003). Shirlaw, et al., (2003) hence used 3% and 2% relative volume losses as upper limits for settlements in Kallang Formation and in other formations, respectively, to evaluate TBM performance in terms of settlement induced over tunnels.

In addition to the settlement monitoring data, 22 incidents of large, localized ground losses were also reported (Shirlaw, et al., 2001). These large, localized ground losses were of two types; 1. subsurface voids, refers to voids which formed above the tunnel face but were grouted before they could migrate to the surface, of which 5 cases were observed, 2. surface sinkholes, refers to local depressions which were found by visual inspection to appear over the tunnels as the machine

advanced (schematic given in Figure 3-5) of which 17 cases were observed. Details of these large, localized ground losses are summarized in Table 3-4. The reason why these ground losses are considered, in addition to the settlement monitoring data is because while involving large volumes, they were highly localized and thus were not reflected in the ground settlement monitoring data (Shirlaw, et al., 2001). An example of a grouted void is depicted in Figure 3-6, and demonstrates the limited plan area of these large ground losses (Shirlaw, et al., 2001).

3.3.2 RESULTS

Table 3-5 combines data from the settlement monitoring program and from observations of large, localized ground losses. A frequency histogram of 617 data points from the settlement monitoring program is given in Figure 3-7. Having earlier established a Relative Volume Loss (RVL) of less than 2% as satisfactory settlement performance of tunneling, Figure 3-7 shows that in 93% of the cases, RVL<2% was obtained, indicating overall reasonably good settlement control during tunneling (Shirlaw, et al., 2001). If we were to organize these numbers by geological formation, as is presented in Figure 3-8, we can see that good settlement control was achieved in most formations, although multiple instances of RVL>2% were observed in three formations, namely the Jurong Formation with overlying Kallang Formation, the Kallang Formation and mixed faces of the two (Shirlaw, et al., 2001).

In order to account for the different tunnel lengths driven in the respective formations (Shirlaw, et al., 2001), the number of cases of RVL>2% and large, localized ground losses were normalized to give the frequency of their occurrence for every km of tunnel driven, and is presented in Figure 3-9. While equal numbers of incidences of large, localized ground losses were obtained in both the mixed grades of Bukit Timah Granite and in the Jurong Formation, the frequency of occurrence was much higher in the former geological formation (Shirlaw, et al., 2001). Figure 3-10 shows a plot of the volumes of these large, localized ground losses, from which it can be

seen that volume losses attributable to launching/docking of the machine and from tunneling in the Jurong Formation were significantly less than that during tunneling in the Bukit Timah Granite.

3.3.3 Influence of Construction Methods on Settlement

Most of the 11.5 km tunneled using TBMs on the NEL was driven using EPB machines (about 10 km), while the remaining distance was driven using open face semi-mechanical shields (Shirlaw, et al., 2003). In this short distance tunneled using open face shields, 7 out of 44 data points of RVL were greater than 2%, and 2 incidences of large, localized ground losses occurred.

Of the two incidences of large localized ground losses, a faulted zone was encountered in one case, resulting in major loss of ground (150 m^3) as the unstable broken rock entered the tunnel, while in the other, material from a steeply dipping bed of completely weathered sandstone raveled as it was encountered in the tunnel face, and required the injection of 25 m^3 of grout for stabilization, and settlement of over 70mm was measured on a bridge located nearby (Shirlaw, et al., 2001). This is similar to what was experienced on the NS-EW line, where large settlements occurred during open face shield tunneling in the Jurong Formation due to the presence of completely weathered rock or faulted zones in the tunnel face.

3.3.4 Influence of Geology on Settlement

Because most of the NEL was tunneled using EPB machines, it presents the unique opportunity to study in detail the performance of EPB tunneling in Singapore. Suwansawat (2002) includes tunnel geometry and depth, geology, face pressures applied, penetration rate, shield inclination, overcutting and tail void grouting in a list of factors which influence settlement during EPB tunneling. Given the available published information, the influence of four factors will be discussed: the relationship between geology and face pressures applied, tail void grouting and launching/docking of the shield.

3.3.4.1 Effect of Applied Face Pressures

While it may not be particularly insightful to simply state that applied face pressures have an effect on settlement, quantifying the amount of face pressure appropriate for different geological formations can lead to a more meaningful discussion. Figures 3-11a to 3-11h are plots of relative volume losses against normalized face pressures applied for different geological formations.

For Bukit Timah Granite, while face pressures in the range of 0.4 to 0.6 times that of overburden pressure were sufficient to control settlements in residual soil (Grade VI) (Figure 3-11a), this face pressure was difficult to sustain in the presence of mixed grades (Figure 3-11b), and resulted in seven incidences of large, localized ground losses (Shirlaw, et al., 2003). Of the seven, five occurred during the South-bound tunnel drive from Serangoon (SER) to Woodleigh (WDL) for Contract 704, with the remaining two occurring on the same contract but in different tunnels. Figure 3-12 contains the geological cross-section of the tunnel drive, face pressures applied and number of skips per ring, which indicates the amount of material being removed per ring (Shirlaw, et al., 2000). Indicated in Figure 3-12 also are the locations and volumes of the five ground losses indicated in red boxes (Shirlaw, et al., 2000). Mixed face conditions between residual soil (Grade VI), completely weathered rock (Grade V) and moderately weathered rock (Grade III) were encountered during the tunnel drive.

As previously discussed in chapter 1, successful usage of Earth Pressure Balance (EPB) to control tunnel face stability depends on the ability of the excavated soil to form an adequate plug (Shirlaw, et al., 2000). While residual soil of Bukit Timah Granite (Grade VI), with its high fines content and low permeability, encounters no difficulty in doing so, the spoil of moderately weathered Bukit Timah Granite (Grade III) has a low fines content and consists mainly of gravel and cobble sized granite fragments, material which cannot form an adequate plug, resulting in losses in face pressures (Shirlaw, et al., 2000). From Figure 3-12, we observe that during the tunneling in moderately weathered (Grade III) Bukit Timah Granite from rings 333 to 383, applied face

pressures dropped to less than ground water pressures, and subsurface voids which required 196 m^3 of grout to fill were formed (Shirlaw, et al., 2000). The presence of mixed face conditions on the same tunnel drive resulted in the formation of another four large, localized ground losses, generally corresponding to low applied face pressures. Applied face pressures remained below ground water pressures from rings 320 to 420. At the same time, the number of skips per ring, was significantly larger than the predicted value of eight skips per ring. From rings 330 to 390, an average of 10.4 skips per ring was recorded, indicating that over-excavation consistently occurred over 60 rings (Shirlaw, et al., 2003).

For the Jurong Formation, differentiating between Jurong Formation with overlying Kallang Formation and Jurong Formation without overlying Kallang Formation was used to indicate differences in weathering extents of the Jurong Formation(Shirlaw, et al., 2003). The deposition of the Kallang Formation soils into eroded channels of the Jurong Formation signals the presence of zones of weaker rock or faulting/folding in the latter formation (Shirlaw, et al., 2003). Settlements were uniformly low when tunneling in the Jurong Formation without overlying Kallang Formation (Figure 3-11d). These settlements were independent of face pressures applied; the surface sinkhole which formed as the tunnel face passed below was due to an old water main breaking (Shirlaw, et al., 2001). Because the main was in poor condition, it was deemed likely that most of the ground loss was due to the bursting of the water main (Shirlaw, et al., 2001). This contrasts with settlements obtained in the Jurong Formation with overlying Kallang Formation (Figure 3-11c), which not only had larger magnitudes of relative volume losses, but also five cases of large, localized ground losses. There were two factors which contributed to these greater settlements, the first being that when the cover to the Kallang Formation was low (less than 3 m), reduced arching ability of the weathered rock led to the magnitude of settlement being controlled by the low strength of soils in the Kallang Formation. The second factor is that weathered Jurong Formation rocks "ravel rapidly under conditions of seepage" and without sufficient face support, a process

exacerbated by the vibrations of the TBM, resulting in significant ground losses (Shirlaw, et al., 2000; Shirlaw, et al., 2003).

For the Kallang Formation, face pressures in the range of 0.9 to 1.2 times that of overburden pressures were required to minimize settlement (Figure 3-11e) (Shirlaw, et al., 2003). The use of jet grouting or some form of ground treatment was effective in controlling settlement in the Kallang Formation for a greater range of face pressures (Shirlaw, et al., 2003). Higher settlements on the whole were obtained on Contract 708, as a result of the TBM operators' decision to apply lower face pressures (Shirlaw, et al., 2003). From Figure 3-11f, it can be seen that tunneling through mixed faces of the Jurong Formation and the Kallang Formation resulted in volume losses of the same order of magnitude as that for the Kallang Formation, suggesting that it was the latter formation which controlled settlement. This is confirmed by the formation of two large, localized ground losses which occurred as the shield drove from a full face of the Jurong Formation into the Kallang Formation, where applied face pressures were inadequate to control the soft soils of the latter formation (Shirlaw, et al., 2003).

Settlement during tunneling in the Old Alluvium was well-controlled and independent of face pressures applied (Figure 3-11g), at least for this project (Shirlaw, et al., 2003). As for tunneling through mixed faces of the Old Alluvium and the Kallang Formation, face pressures of 0.8 to 1.2 times that of overburden were employed successfully to minimize settlements (Figure 3-11h), which is similar to that recommended for settlement control in the Kallang Formation. Shirlaw, et al., (2003) suggest that it is the more deformable soils of the Kallang Formation which control settlement in this case, similar to what was experienced during tunneling through mixed faces of the Jurong Formation and the Kallang Formation.

As much as settlement control is an important factor in the TBM operator's decision of face pressures to apply, it is not the only consideration. While it is possible to operate the TBM under full face pressure in the known presence of buried valleys/mixed face conditions in an attempt to

mitigate ground losses arising from the increased likelihood of a weaker material in the tunnel face, TBM operators are sometimes reluctant to do so because fully pressurized machining in the stronger, less weathered material can generate excessive amounts of heat and wear on the drill bits (Shirlaw, et al., 2000). In this way, TBM operators have to balance the trade-offs that come with controlling settlement and the amount of heat and abrasion (which affects amount of maintenance and downtime required) that therefore arises from fully pressurized face tunneling.

3.3.4.2 Effect of Tail Void Grouting

A tail void is an annulus that forms outside of the installed tunnel lining as the shield advances and a schematic of its formation is given in Figure 3-13 (Maidl, et al., 1996; Suwansawat & Einstein, 2006). Figure 3-14 proposes some scenarios which affect the size of this annulus (Maidl, et al., 1996). Grouting of the tail void is required to minimize settlement caused by movement of ground onto the tunnel lining, (Suwansawat & Einstein, 2006).

Prior to NEL construction, which has seen the most extensive use of EPB tunneling in Singapore to date, EPB machines on the NS-EW line and in sewer construction were employed to control settlements in the Kallang Formation. It was recommended, given the experience on those projects, that all EPB machines be equipped for simultaneous tail void grouting to minimize settlements resulting from any delays in grouting the tail voids (Ow, et al., 2004). Shirlaw, et al., (2001) propose that this, combined with appropriate face pressures, should be effective in keeping relative volume losses less than 2%. The effect of tail void grouting on settlement can be observed from Figure 3-11e. Despite blockage in the tail void grout pipe, the TBM operator decided to continue tunneling, which resulted in Relative Volume Loss of 5%, twice that normally experienced on the same contract with similar applied face pressures (Shirlaw, et al., 2003).

3.3.4.3 Effect of Machine Launching/Docking

From seven tunneling projects in Singapore and Canada, it was found that launching of the shield was a significant factor in the formation of large, localized ground losses, contributing to 10 out of 57 total incidents considered (Shirlaw, et al., 2005). For NEL tunneling, two incidences of large, localized ground losses occurred during the launching of the machine, with interesting circumstances in both cases worthy of further discussion.

During launching in the Jurong Formation (details given in Figure 3-15), highly weathered mudstone, which was possibly mixed with lean concrete that was used for ground treatment, "plugged" the center of the chamber (Shirlaw, et al., 2003). This plug restricted the advance of the shield, while excavation of the surrounding weak rock continued, leading to over-excavation (Shirlaw, et al., 2003). A schematic of this process and a picture of a plug (formed on a different project) are given in Figures 3-16 and 3-17, respectively. As for the second case which was launched in the Kallang Formation (details given in Figure 3-18), size differences between the cutterhead and tail skin resulted in an annulus around the shield, which was sealed using a rubber seal (Shirlaw, et al., 2003). Before the tailskin could tunnel past the diaphragm wall, which would have allowed it to erect and grout the first ring, the rubber seal broke, causing fluvial sands under water pressures of 150kPa to enter the launch area, resulting in the formation of a 30 m^3 surface sinkhole (Shirlaw, et al., 2003).

Large, localized ground losses occurred during docking due to a combination of insufficient ground treatment/support in the docking area and reduction in face pressures as the machine approached the docking station (Shirlaw, et al., 2003).

3.3.5 Comparison with Case Studies from Other Projects

One of the cases of surface sinkholes which took place in the Jurong Formation during NEL tunneling was due to an old water main breaking as the tunnel face passed below (Shirlaw, et al.,

2001). Because the main was in poor condition, it was deemed likely that most of the ground loss was due to the bursting of the water main (Shirlaw, et al., 2001). This is somewhat reminiscent of the experience during tunneling for the Porto Metro, Portugal, where old wells and their accompanying handmade water tunnels or 'minas' form preferential pathways for groundwater flow, and cause large settlements when encountered (Sousa, 2010). The presence of man-made structures, such as sheet piles which were encountered during Circle Line tunneling, had a similar effect (Osborne, et al., 2008).

3.4 Settlement Measured for the Circle Line (CCL)

The use of Earth Pressure Balance (EPB) tunneling on the North-East line (NEL) which resulted in large, localized ground losses could have influenced the choice of construction methods employed on the Circle Line (CCL) (Osborne, et al., 2008). While distances tunneled by EPB machines on the CCL exceed distances tunneled on the NEL by EPB machines (shown in Figures 1-10 and 1-11), a greater proportion of slurry machines were employed on the CCL to possibly provide better control of face stability given that the slurry acts to instantaneously increase face pressures (Osborne, et al., 2008). The usage of slurry machines, however, has the added complication of having to design an appropriate slurry mix and a production and delivery system capable of both delivering effective face pressure to the tunnel and recycling and processing the slurry (Osborne, et al., 2008).

Unfortunately, increased employment of slurry machines could not eliminate the problems with large localized ground losses, which were observed mainly in three geological conditions: mixed weathering grades of the Bukit Timah Granite, weathered Jurong Formation and in mixed face conditions between the Jurong Formation and the Kallang Formation (Osborne, et al., 2008). These three formations also accounted for most of the large, localized ground losses which formed during NEL tunneling. Additional problems with slurry/foam discharge at surface were

encountered during CCL tunneling, as shown in Figure 3-19 (Osborne, et al., 2008). The discharge of slurry to the surface occurred in weathered Jurong Formation, where the spoil formed was a "sticky clay" that increased the probability of clogging in the suction entry gate area (Osborne, et al., 2008; Shirlaw & Hulme, 2008). Clogging in the suction entry gate area severed the connection between the plenum and excavation chambers, and affected the machine's ability to control face pressures applied in the excavation chamber (Shirlaw & Hulme, 2008). This resulted in excavation chamber pressures to increase uncontrollably, which coupled with high flow rates of highly pressured slurry, caused migration of slurry to the surface (Shirlaw & Hulme, 2008). The discharge of slurry to the surface, while it poses less risk to surface structures, still presents a road hazard and a disruption to surface activities (Osborne, et al., 2008).

Table 3-1: Surface settlements due to tunneling for North-South East-West (NS-EW) line (Hulme & Burchell, 1992)

TABLE 7. Settlements

Tunneling methods (1)	Kallang formation (marine clays/fluvial sands) (2)	Jurong formation (weathered to fresh sedimentaries) (mm) (3)	Bukit Timah formation (completely weathered/granite) (mm) (4)
Greathead shield	NA	10–200 (C106), 10–350 (C109)	10–45 (C105)[a], 10–60 (C106)
Greathead shield and compressed air	30–100 (C104), 20–60 (C301)	5–15 (C301), 100 (C109), 20 (C107)[b]	5–40 (C104)
Greathead shield and ground treatment	100–200 (C106)	NA	NA
Greathead shield with ground treatment and compressed air	30–60 (C108)	NA	NA
Tunnel-boring machine	NA	NA	50–300 (C105)[a]
Tunnel-boring machine with compressed air	200–400 (C105)	NA	20–120 (C105)
Earth-pressure balanced shield	60–120 (C301)	NA	NA
New Austrian tunneling method	NA	5–20 (C104), 5–10 (C107B), 20–60 (C107A)[c]	10–20 (C105)[a]
New Austrian tunneling method in compressed air	NA	NA	10–100 (C104)

[a]Single tunnel.
[b]Four tunnels.
[c]Twin tunnels, one vertically above the other.
Note: Settlements are for twin tunnels, side by side unless noted otherwise; NA = not applicable.

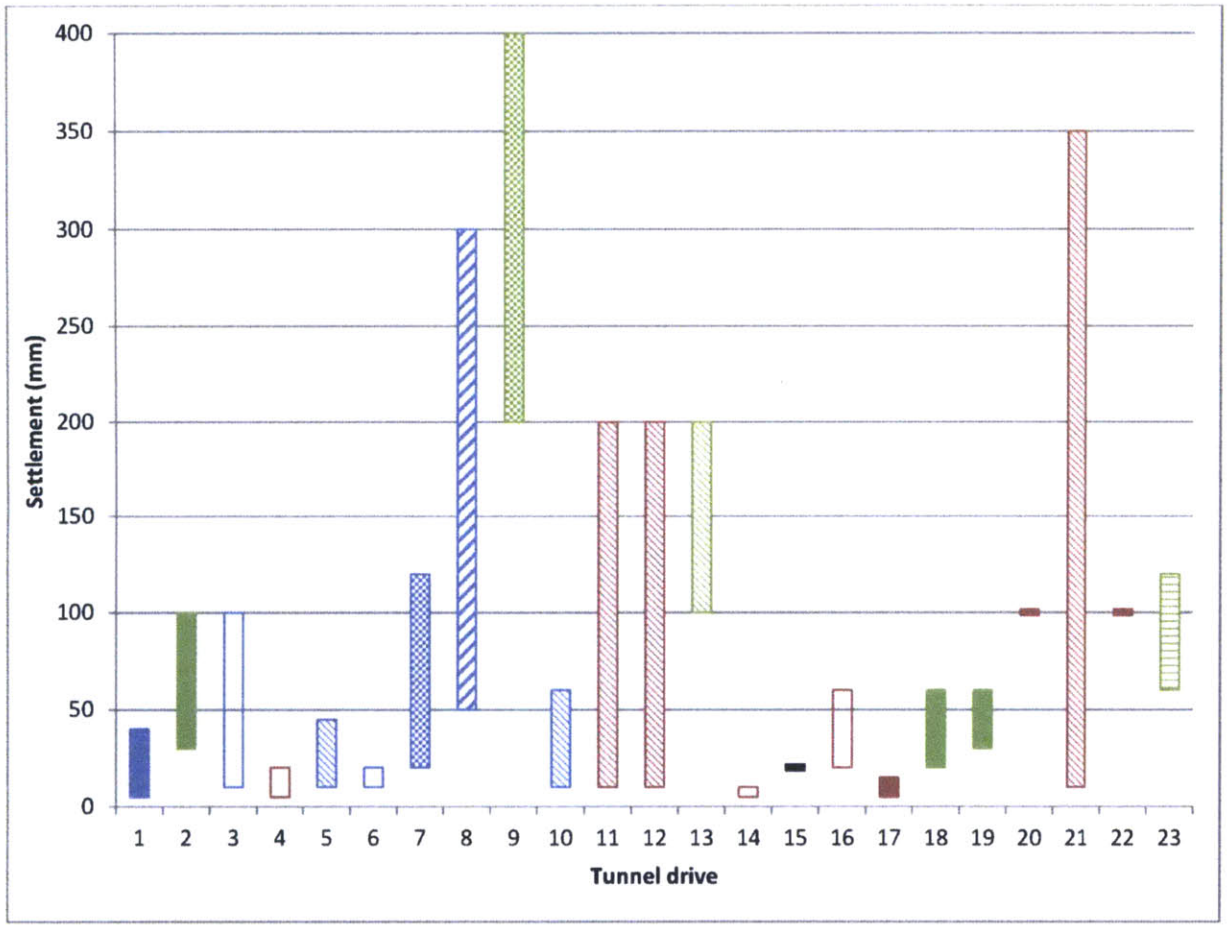

No.	Contract no. & drive
1	C104 TAP-NOV
2	
3	
4	
5	C105 ORC-SOM(NB)
6	
7	C105 ORC-NEW C105 ORC-SOM(SB)
8	
9	
10	C106 DBG-SOM
11	
12	C106 DBG-CTH
13	
14	
15	C107 RFP-CTH
16	C107A RFP-C301
17	C107A/C301 CTH-BGS
18	
19	C108 TPG-RFP
20	C109 OTP-TPG
21	C109 TIB-OTP
22	
23	C301 LVR-BGS

Legend					
	Bukit Timah Granite		Shield in comp. air		NATM
	Jurong Formation		Shield in free air		EPB
	Kallang Formation		TBM in comp. air		
	Old Alluvium		TBM in free air		

Figure 3-1: Surface settlements for NS-EW line, organized by tunnel drive (Hulme & Burchell, 1992)

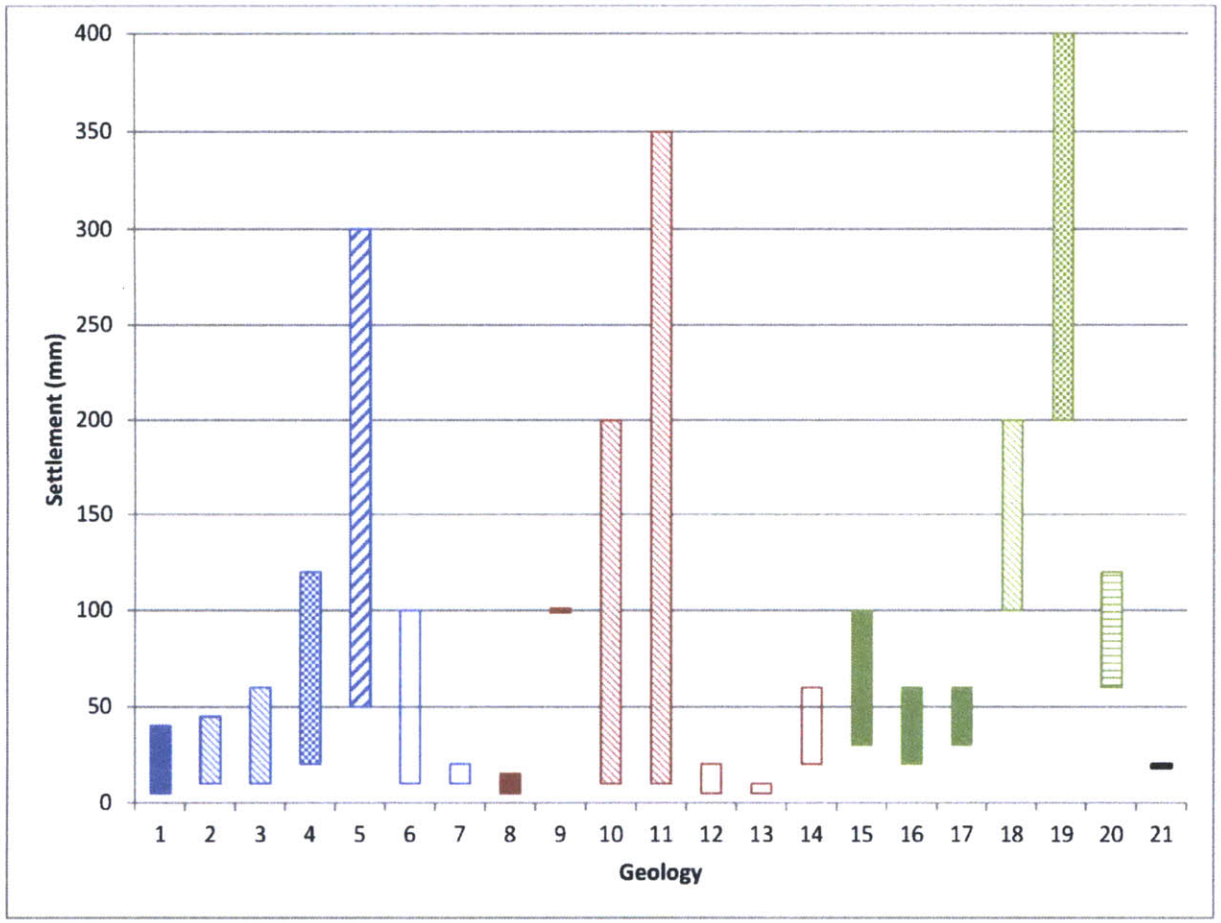

No.	Contract no. & drive
1	C104 TAP-NOV
2	C105 ORC-SOM(NB)
3	C106 DBG-SOM
4	C105 ORC-NEW
5	C105 ORC-SOM(SB)
6	C104 TAP-NOV
7	C105 ORC-SOM(NB)
8	C107A/C301 CTH-BGS
9	C109 OTP-TPG C109 TIB-OTP
10	C106 DBG-SOM C106 DBG-CTH
11	C109 TIB-OTP
12	C104 TAP-NOV
13	C106 DBG-CTH
14	C107A RFP-C301
15	C104 TAP-NOV
16	C107A/C301 CTH-BGS
17	C108 TPG-RFP
18	C106 DBG-CTH
19	C105 ORC-NEW C105 ORC-SOM(SB)
20	C301 LVR-BGS
21	C107 RFP-CTH

Legend					
	Bukit Timah Granite		Shield in comp. air		NATM
	Jurong Formation		Shield in free air		EPB
	Kallang Formation		TBM in comp. air		
	Old Alluvium		TBM in free air		

Figure 3-2: Surface settlements for NS-EW line, organized by geology (Hulme & Burchell, 1992)

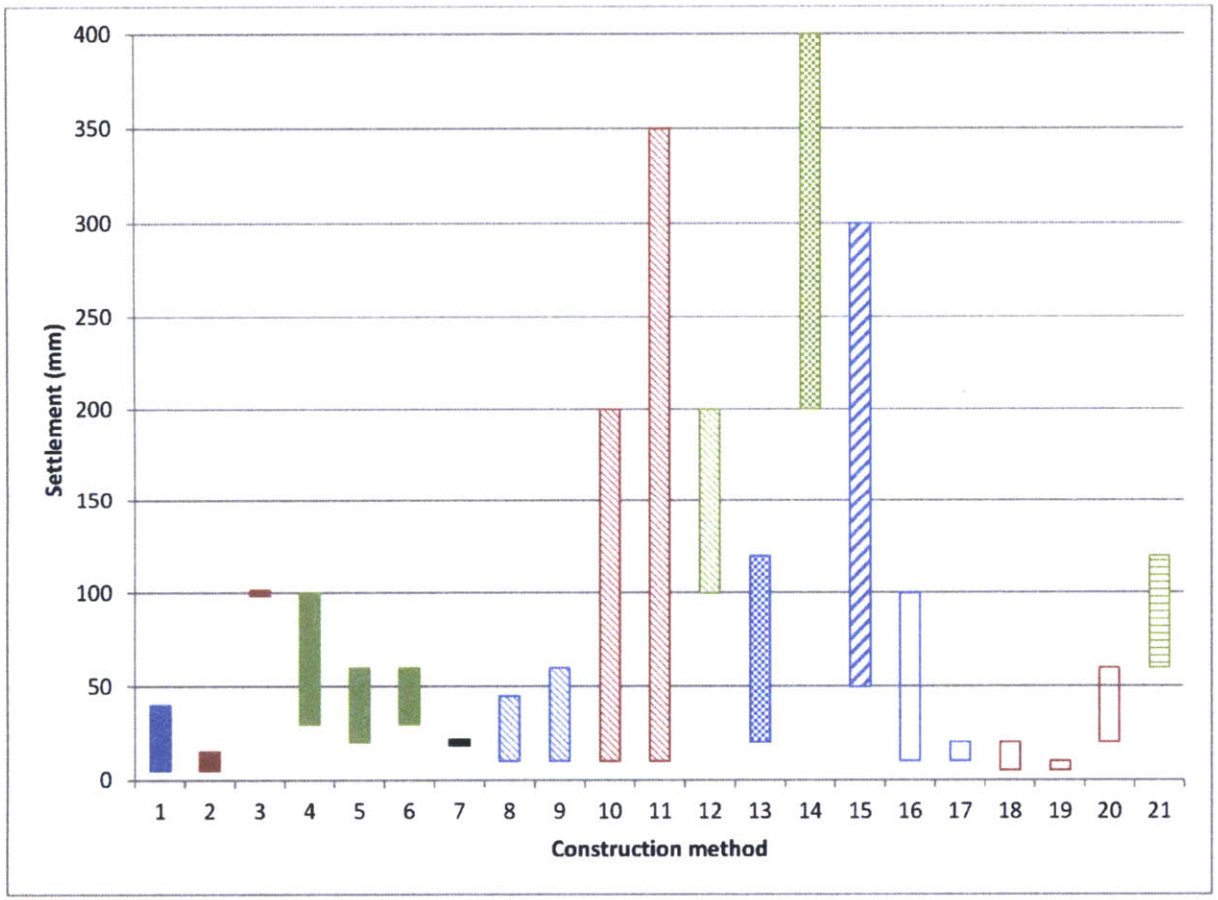

No.	Contract no. & drive
1	C104 TAP-NOV
2	C107A/C301 CTH-BGS
3	C109 OTP-TPG C109 TIB-OTP
4	C104 TAP-NOV
5	C107A/C301 CTH-BGS
6	C108 TPG-RFP
7	C107 RFP-CTH
8	C105 ORC-SOM(NB)
9	C106 DBG-SOM
10	C106 DBG-SOM C106 DBG-CTH
11	C109 TIB-OTP
12	C106 DBG-CTH
13	C105 ORC-NEW
14	C105 ORC-SOM(SB)
15	
16	C104 TAP-NOV
17	C105 ORC-SOM(NB)
18	C104 TAP-NOV
19	C106 DBG-CTH
20	C107A RFP-C301
21	C301 LVR-BGS

Legend					
	Bukit Timah Granite		Shield in comp. air		NATM
	Jurong Formation		Shield in free air		EPB
	Kallang Formation		TBM in comp. air		
	Old Alluvium		TBM in free air		

Figure 3-3: Surface settlements for NS-EW line, organized by construction method (Hulme & Burchell, 1992)

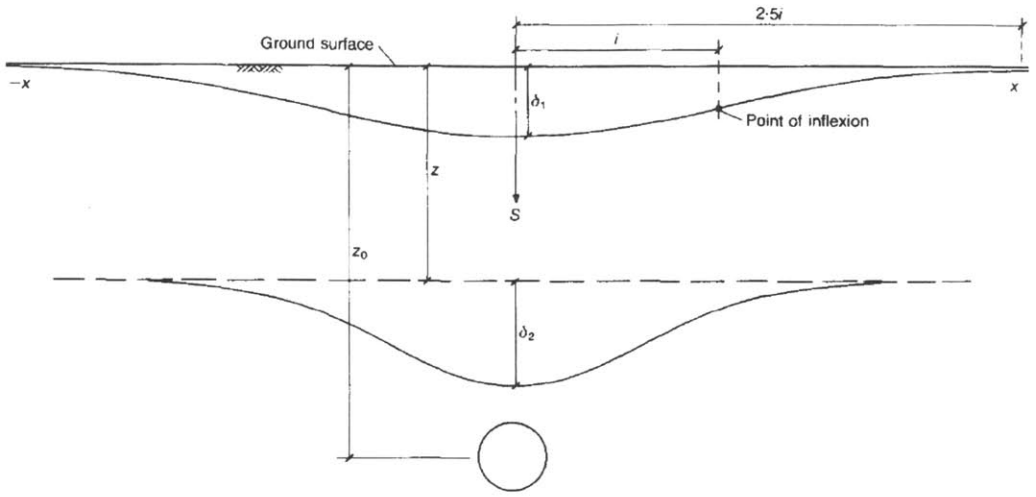

Figure 3-4: Surface and subsurface settlement troughs over tunnels (Mair, et al., 1993, Figure 2)

Table 3-2: Typical values for K (LTA, 2010, Table 20.1)

Formation	**Weathering grade/material**	**Tunneling method**	**K**
Jurong Formation	S(V)/S(VI)	Greathead shield	0.45
	S(V)/S(VI)	Greathead shield in compressed air	0.45
	S(II)/S(III)	EPB shield	0.45
	S(II)/S(III)	NATM	0.45
	FCBB	NATM	0.45 – 0.50
	FCBB	Greathead shield	0.50
Bukit Timah Granite	G(V)/G(VI)	Greathead shield	0.45
	G(V)/G(VI)	Greathead shield in compressed air	0.45
	G(V)/G(VI)	TBM in compressed air	0.45
	G(V)/G(VI)	NATM in compressed air	0.45
	G(V)/G(VI)	EPB shield	0.45
Old Alluvium	-	EPB shield	0.45
Kallang Formation	Marine clay	Semi-blind/semi-mechanical shield	0.50
	Marine clay	Greathead shield with ground treatment and compressed air	0.50
	Marine clay	TBM in compressed air	0.50
	Marine clay	EPB shield	0.50

Table 3-3: K values used (Shirlaw, et al., 2001, Table 2)

Formation	**Weathering grade/material**	**K**
Jurong Formation	All grades	0.50
	FCBB	0.45
Bukit Timah Granite	G(VI)	0.45
	G(I) to G(V)	0.50
Old Alluvium	-	0.50
Kallang Formation	-	0.30

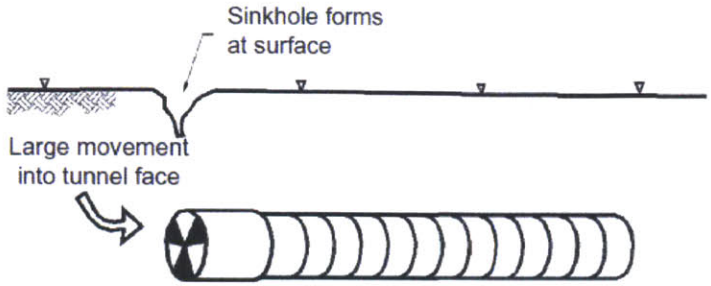

Figure 3-5: Schematic of surface sinkhole formation (Shirlaw, et al., 2003)

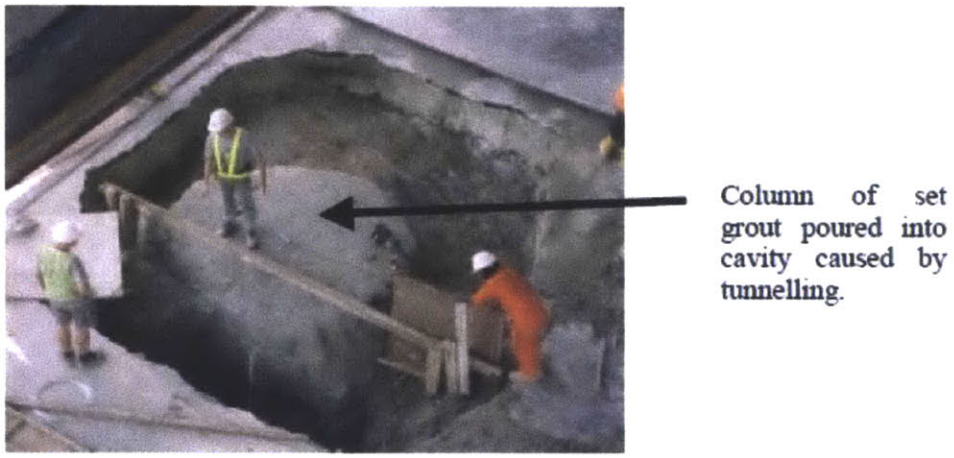

Figure 3-6: Example of large, localized ground loss obtained during NEL tunneling (Shirlaw, et al., 2001)

Table 3-4: Large, localized ground losses encountered during NEL tunneling (Shirlaw, et al., 2001, Table 5)

Construction method		Contract	Drive		Bound	Ring no	Geological Formation	Subsurface void (V)/ surface sinkhole (S)	Size of depression		
									Depth (m)	Area (m^2)	Vol. (m^3)
OFSM		C708	CQY	DBG	N	525-545	JF (no KF above)	V			150
		C708	CQY	DBG	N	636	JF (no KF above)	S	0.1		25+
EPB	Launching	C710	OTP	CNT	N	T8	JF (KF above)	V			20
		C705	PTP	WDL	S	T6	Kallang Formation	S	3		30
	Docking	C710	OTP	HBF	N	1801	JF (KF above)	S	0.5	1m cone	0.13*
		C710	OTP	CNT	N	330	Mixed face: JF/KF	S	0.5	Widespread	
		C705	PTP	WDL	S	330	Old Alluvium	S			15
	Tunneling	C704	SER	WDL	S	333-383	BTG (GIII)	V			196
		C704	SER	WDL	S	324	BTG (GIII/GVI)	V			46
		C704	SER	WDL	S	332	BTG (GIII/GVI)	V			96
		C704	SER	WDL	S	384	BTG (GIII/GVI)	S			67
		C704	SER	WDL	S	384	BTG (GIII/GVI)	S			33
		C704	SER	WDL	N	343	BTG (GIII/GVI)	S			50
		C704	SER	KVN	S	263	BTG (GIII/GVI)	S	0.2	7.07	1.4*
		C708	CQY	CNT	N	240	Mixed face: JF/KF	S	0.25		1
		C710	OTP	HBF	S	60	JF (KF above)	S	1.5	20	30
		C710	OTP	HBF	S	399	JF (KF above)	S	0.6	Extent unknown	
		C710	OTP	HBF	S	464	JF (KF above)	S	0.16		
		C710	OTP	HBF	S	787	JF (KF above)	S	0.5	3m cone	1.18*
		C710	OTP	HBF	N	976	JF (KF above)	S	0.6	1m cone	0.13*
		C710	OTP	HBF	N	1292	JF (no KF above)	S	0.25	20	5*
		C710	OTP	CNT	N	304	Mixed face: JF/KF	S	0.25	Widespread	

JF: Jurong Formation; KF: Kallang Formation; BTG: Bukit Timah Granite; GIII: moderately weathered BTG; GIII/GVI: mixed face conditions between moderately weathered BTG and residual soil

*estimated from depth and area of depression; +estimated from volume of grout used

Table 3-5: No. of cases of >2% Relative Volume Loss and large, localized ground losses, organized by geological formation (Shirlaw, et al., 2001; Shirlaw, et al., 2003)

Formation	EPB			OFSM		
	Total	RVL> 2%	Large, localized ground losses	Total	RVL> 2%	Large, localized ground losses
BTG (residual soil)	43					
BTG (mixed grades)	18	1	7			
JF (KF above)	48	11	7	65	7	
JF (no KF above)	67		1	42		2
FCBB	7			25		
KF	39	14	1			
JF/KF	16	10	3			
OA	231		1			
OA/KF	16	1				
Total	485	37	20	132	7	2

EPB: Earth Pressure Balance machine; OFSM: open face semi-mechanical machine;
RVL: Relative volume loss; BTG: Bukit Timah Granite; JF: Jurong Formation;
FCBB: Fort Canning Boulder Bed; JF/KF: mixed face of JF and KF; KF: Kallang Formation;
OA: Old Alluvium; OA/KF: Mixed face of Old Alluvium and Kallang Formation

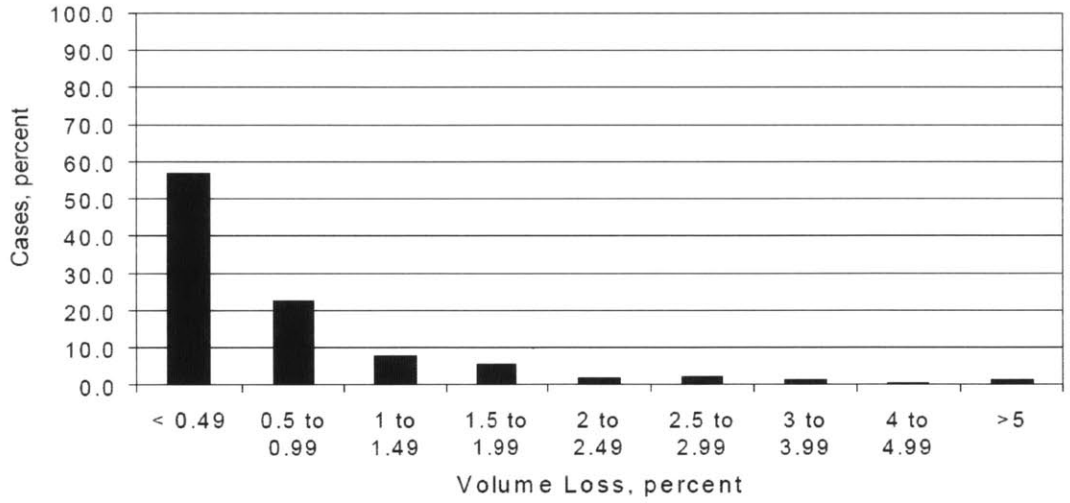

Figure 3-7: Distribution of relative volume loss obtained from settlement monitoring (Shirlaw, et al., 2001)

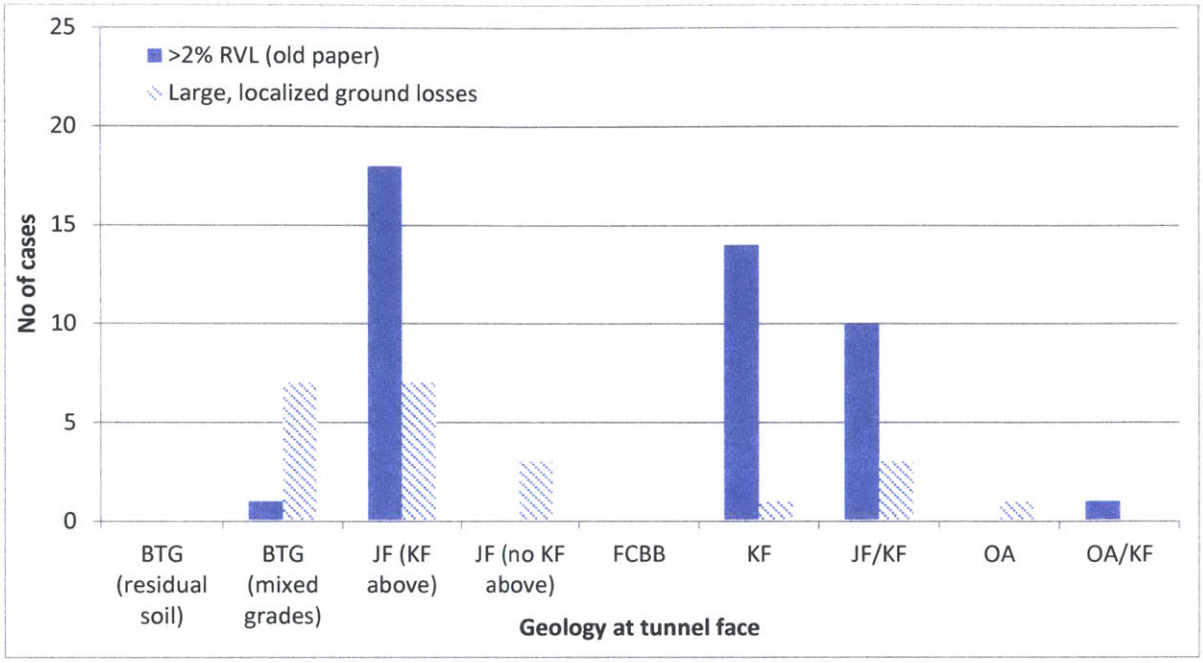

Figure 3-8: Plot of no. of cases of >2% Relative Volume Loss and large, localized ground losses, organized by geological formation

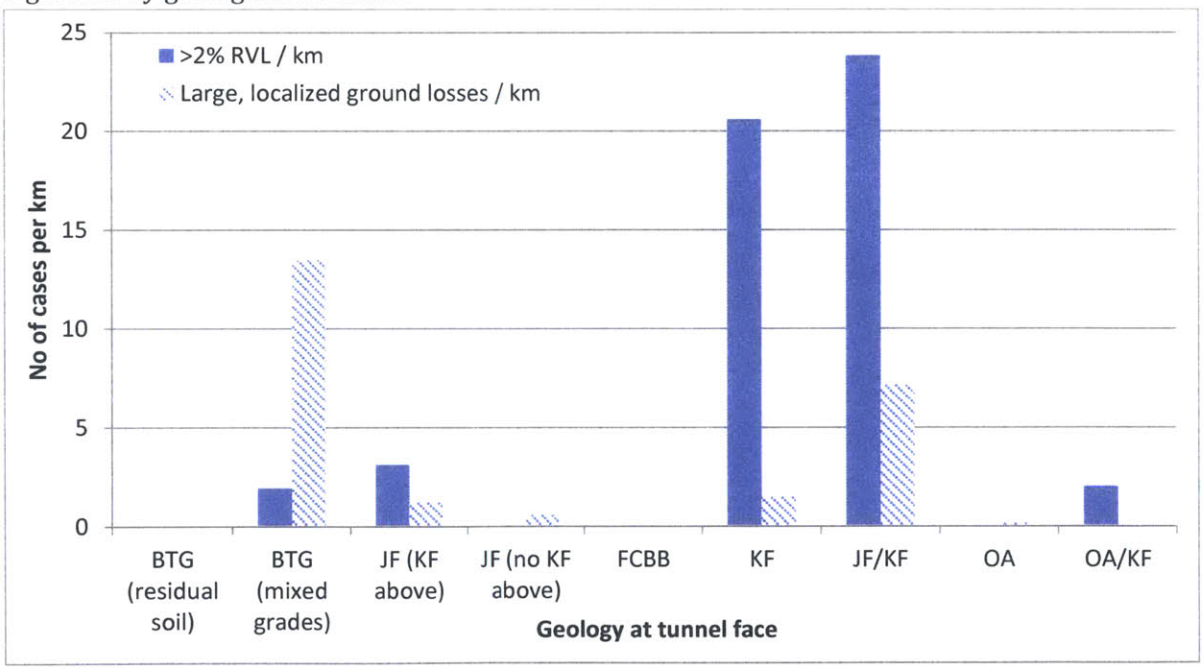

Figure 3-9: Plot of no. of cases of >2% Relative Volume Loss and large, localized ground losses, normalized by distance driven and organized by geological formation

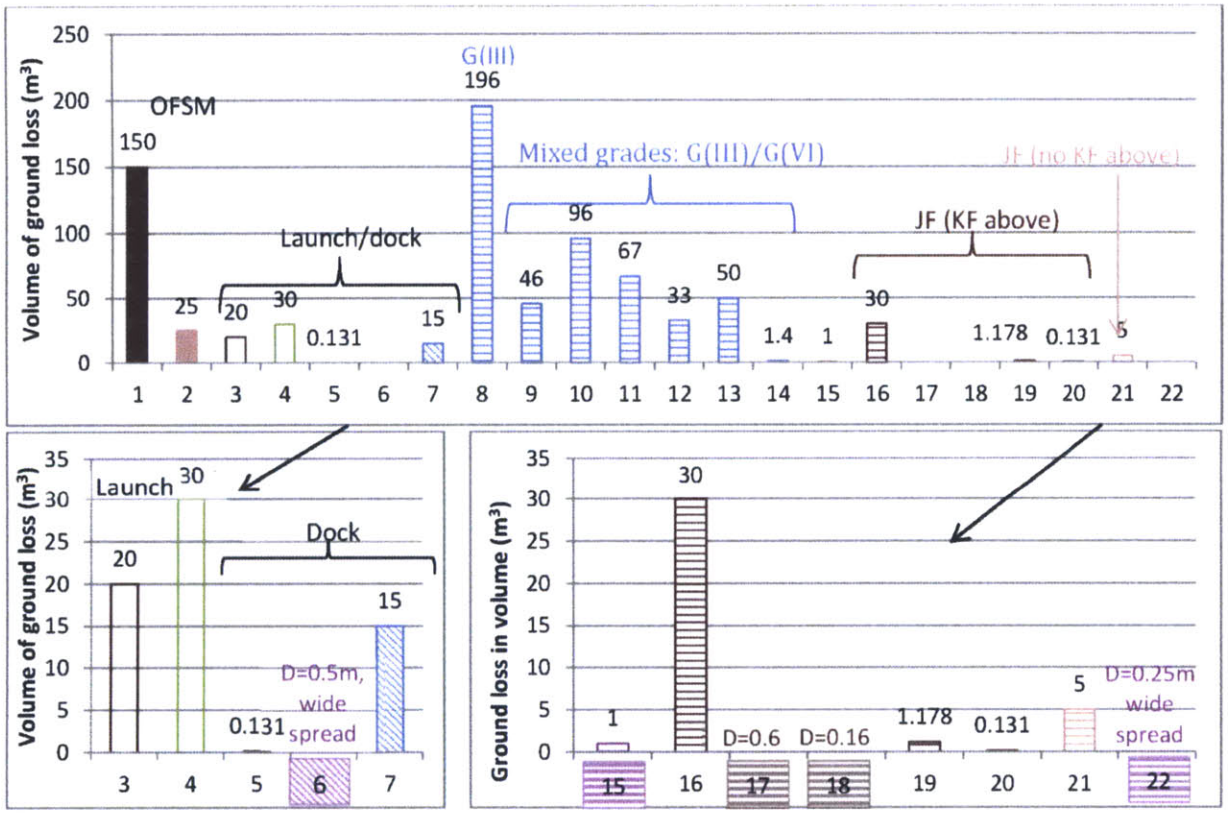

No.	Contract no. & drive
1	C708 CQY-DBG (N)
2	
3	C710 OTP-CNT (N)
4	C705 PTP-WDL (S)
5	C710 OTP-HBF (N)
6	C710 OTP-CNT (N)
7	C705 PTP-WDL (S)
8	C704 SER-WDL (S)
9	
10	
11	
12	
13	C704 SER-WDL (N)
14	C704 SER-KVN(S)
15	C708 CQY-CNT (N)
16	C710 OTP-HBF (S)
17	
18	
19	
20	C710 OTP-HBF (N)
21	
22	C710 OTP-CNT (N)

Bukit Timah Granite	Open Face Semi-Mechanical machine
JF: Jurong Formation (KF above)	Launching
JF: Jurong Formation (no KF above)	Docking
Kallang Formation	During tunneling
Mixed face: JF/KF	

Figure 3-10: Plot of the volumes of large, localized ground losses during NEL tunneling (Shirlaw, et al., 2001; Shirlaw, et al., 2003)

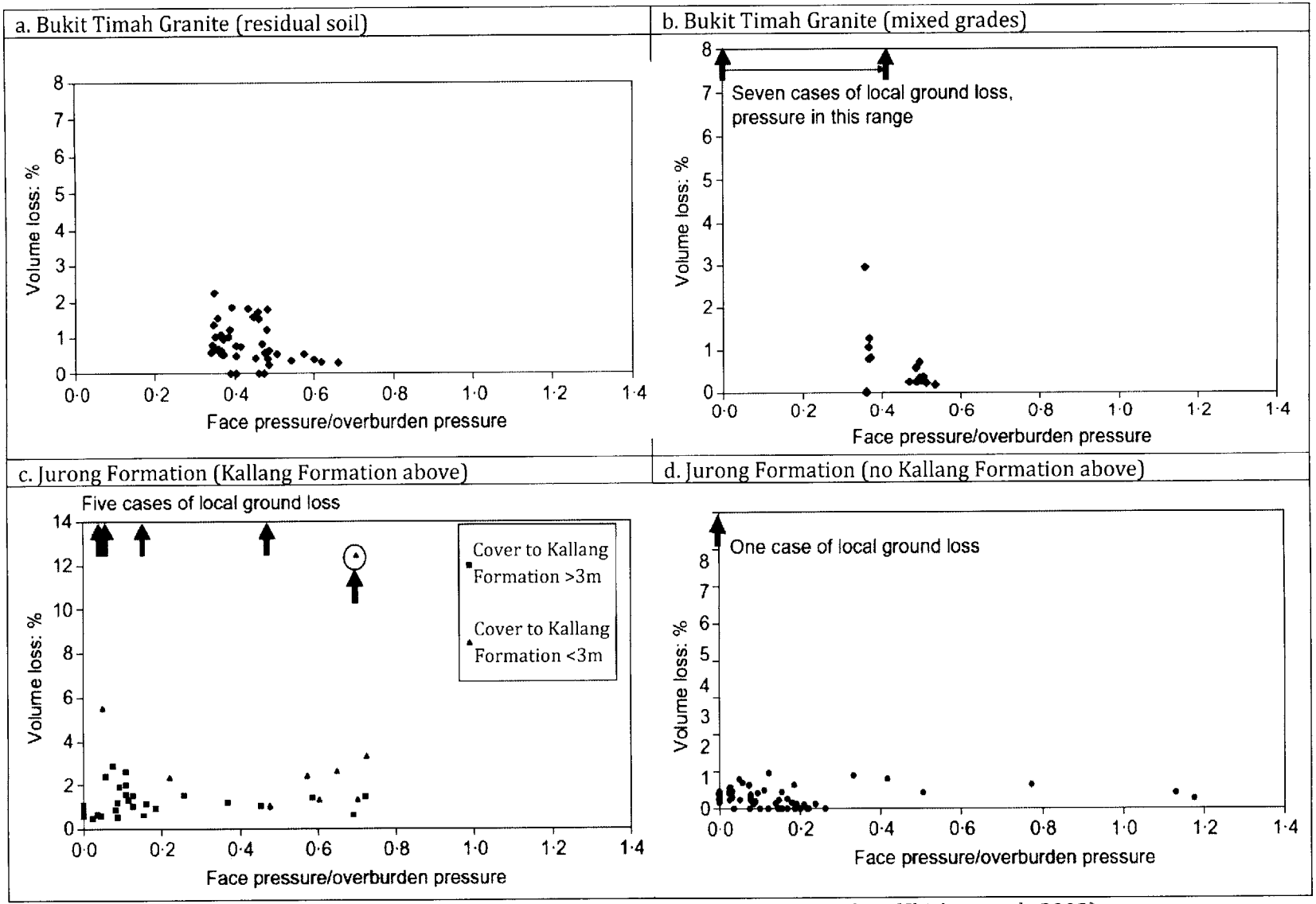

Figure 3-11: Relative volume losses against normalized face pressures during NEL tunneling (Shirlaw, et al., 2003)

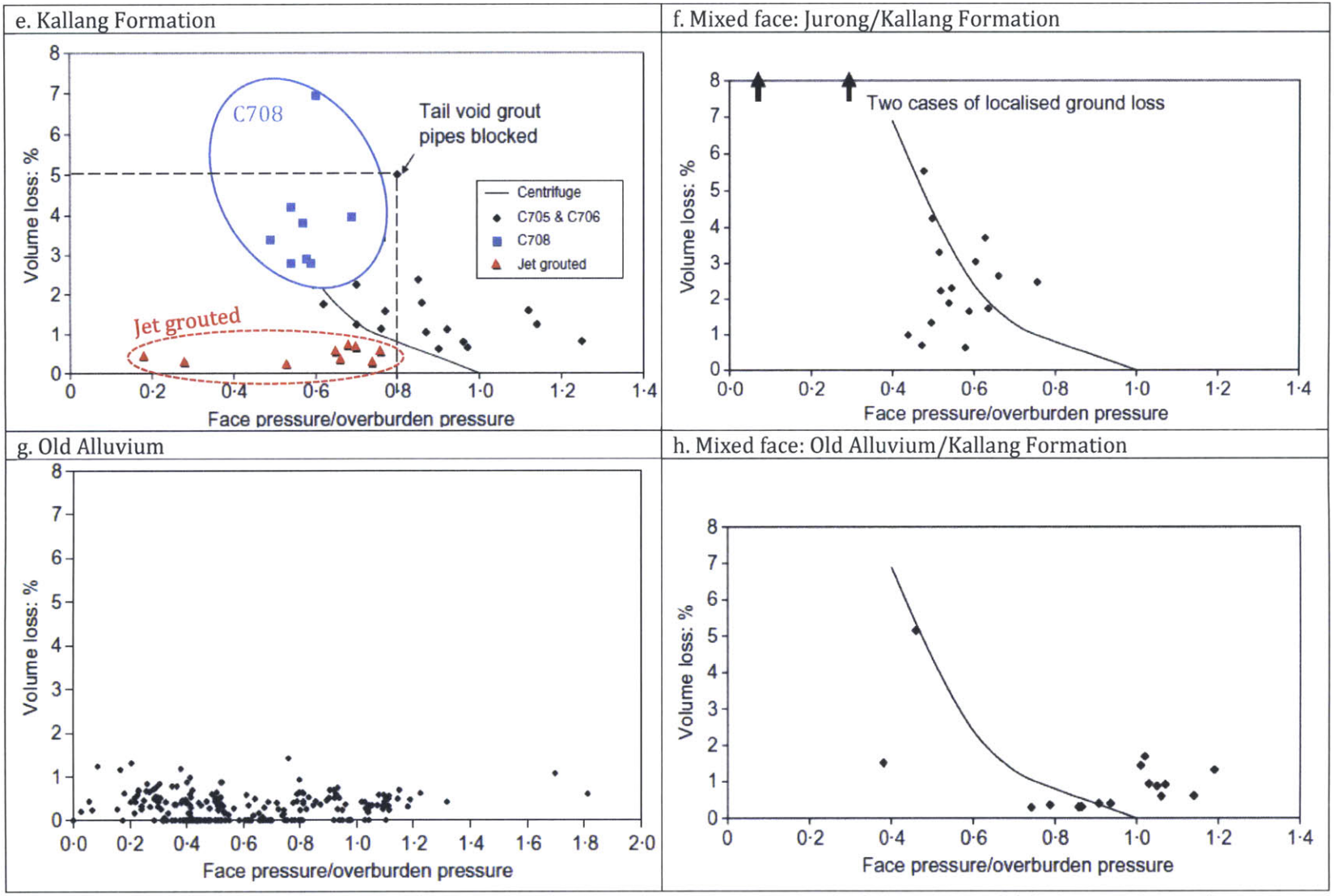

Figure 3-11: Relative volume losses against normalized face pressures during NEL tunneling, continued (Shirlaw, et al., 2003)

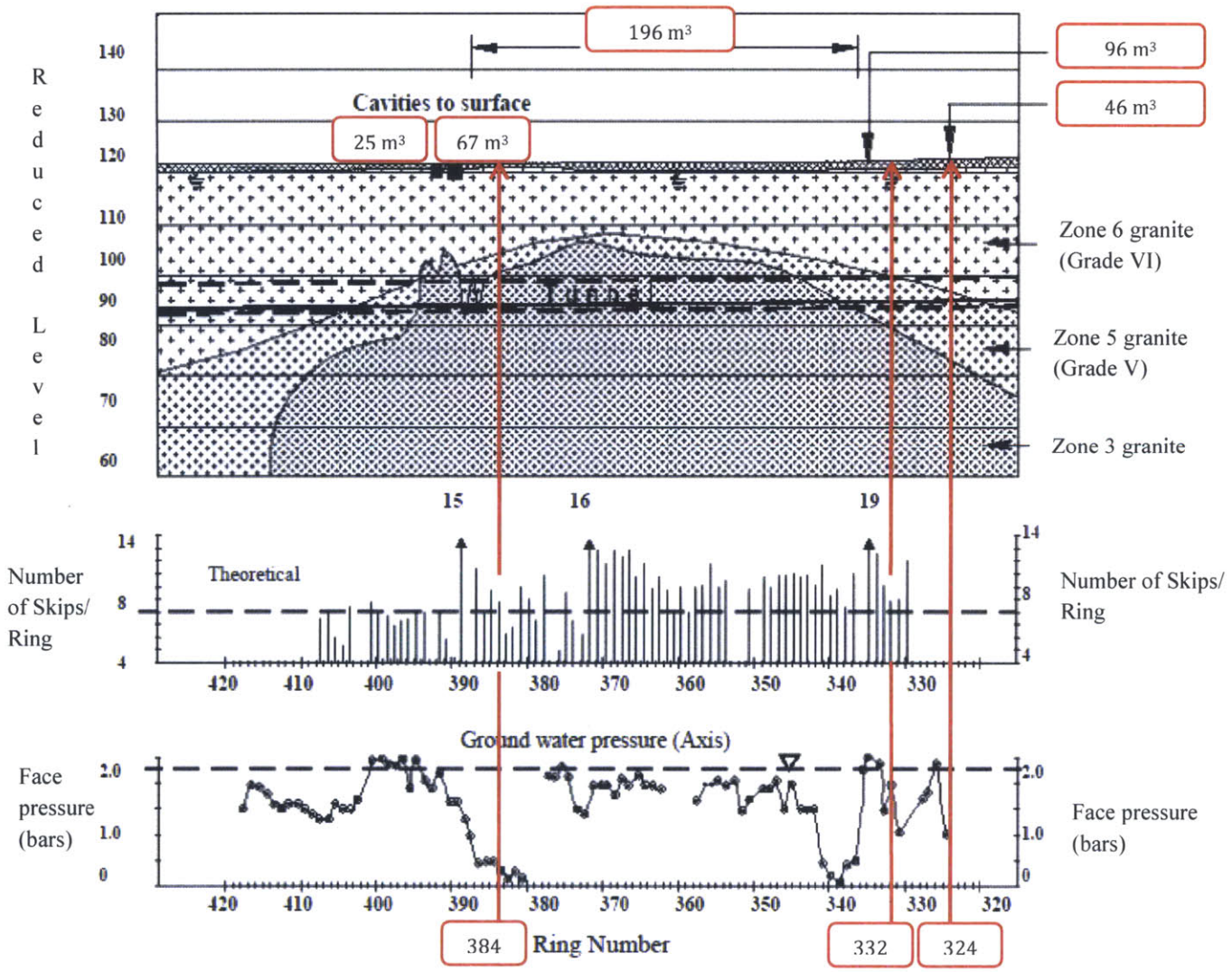

Figure 3-12: Large, localized ground losses induced as a result of loss of face pressure when tunneling through mixed grades of Bukit Timah Granite (NEL) (Shirlaw, et al., 2000)

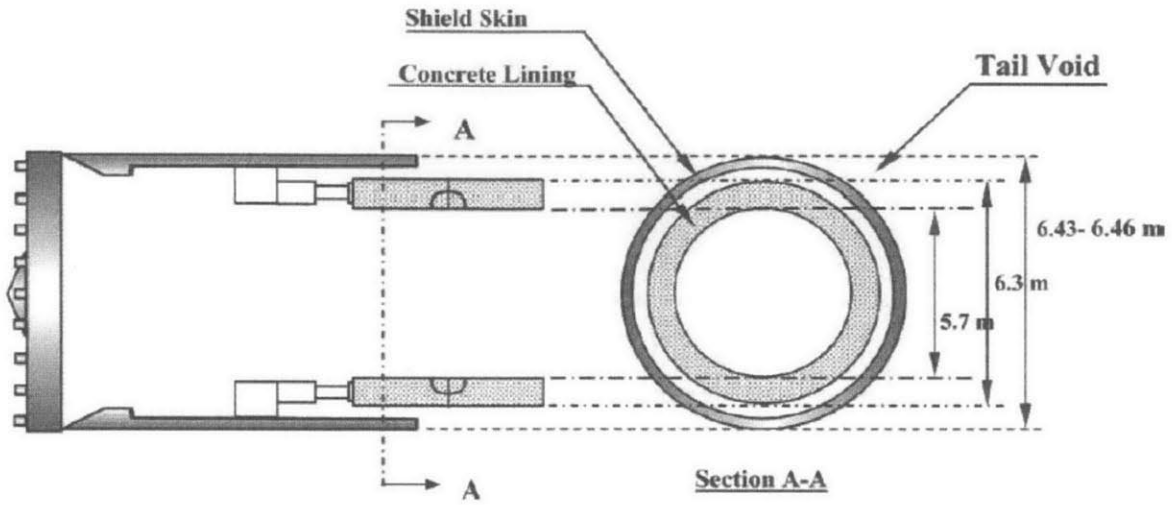

Figure 3-13: Schematic of formation of tail void (Suwansawat & Einstein, 2006)

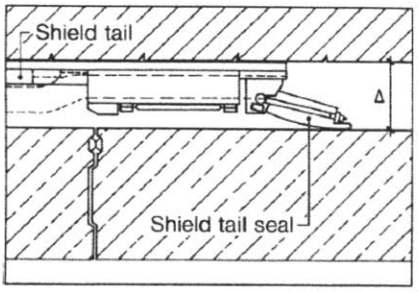

Annular gap due to the thickness of the shield tail metal and the construction of the shield tail seal

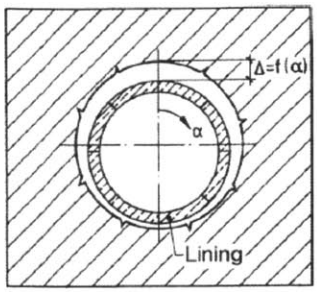

Alteration of the annular gap thickness due to the eccentricity of the lining

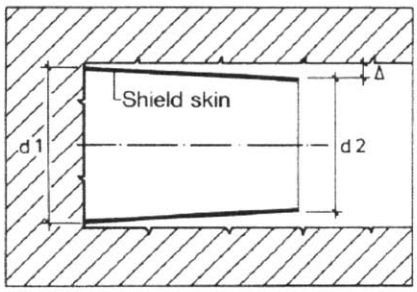

Annular gap due to the taper of the shield skin

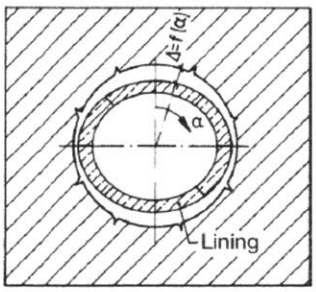

Alteration of the annular gap thickness due to deformation of the lining

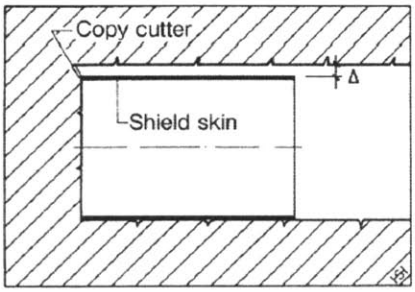

Annular gap due to eccentric overcut

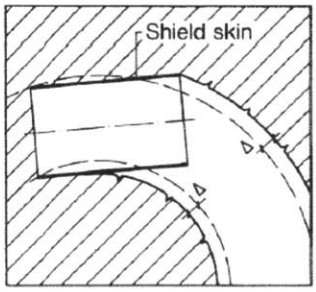

Annular gap due to ground displaced by driving a curve

Figure 3-14: Conditions leading to formation of annulus between shield and ground (Maidl, et al., 1996)

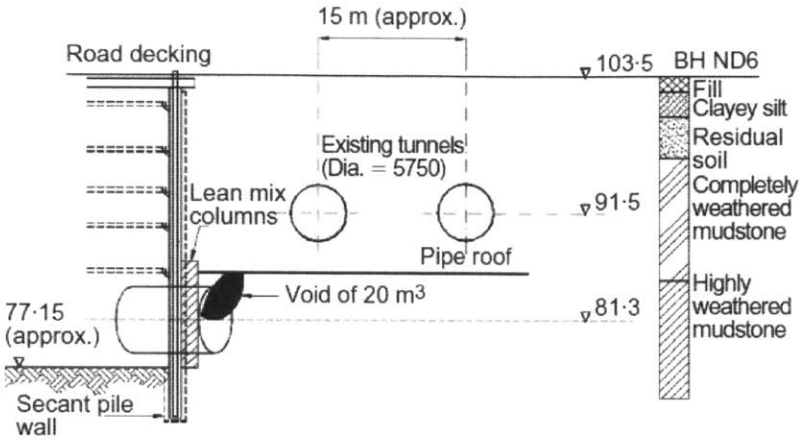

Figure 3-15: Schematic of subsurface void formation during launching of machine in the Jurong Formation

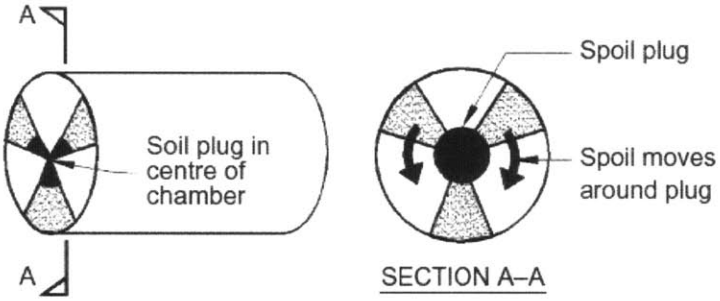

Figure 3-16: Schematic of the formation of plug in center of chamber

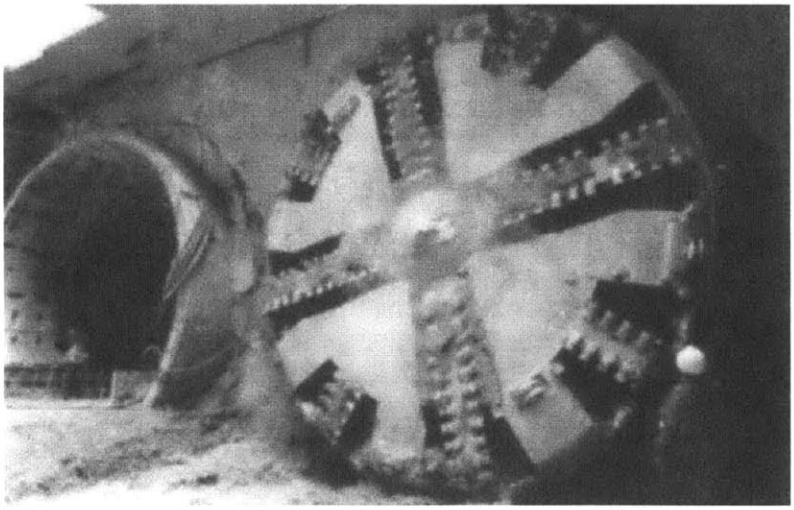

Figure 3-17: Picture of plug formed in center of chamber

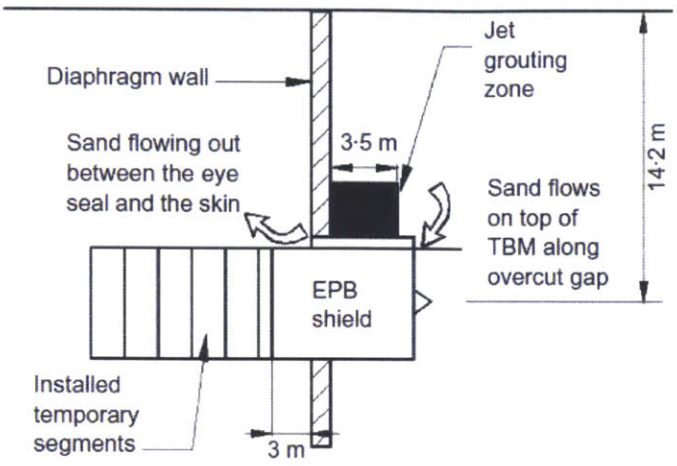

Figure 3-18: Schematic of surface sinkhole formation during launching of machine in the Kallang Formation

Figure 3-19: Discharge of slurry to surface (Shirlaw & Hulme, 2011)

4. CONCLUSION AND RECOMMENDATIONS

Four lines of Singapore's Mass Rapid Transit (MRT) network have been constructed; during tunneling for these four lines, all four major geological formations were encountered. Tunneling in Singapore is characterized by rapidly changing ground conditions, either due to changing geological formations, and/or varying properties within a single geological formation caused by tropical weathering. The test of successful tunneling lies not only in appropriate selection of a Tunnel Boring Machine (TBM) that will perform best in these changing ground conditions, but also in appropriate operation of the TBM. It is the combination of both the given conditions (as in encountered geology) and the adopted solutions (as in adopted construction methods) that ultimately influence settlement, which in turn indicates the ability of the adopted solutions to address the existing geological conditions.

Settlement values for the NS-EW line were reported as a range for separate contracts, while settlement values for the NEL were reported both in the form of calculated Relative Volume Losses (RVL) and individual incidences of large, localized ground losses. These large, localized ground losses were either 1. subsurface voids that formed above the tunnel face but were grouted before migration to the surface, or 2. surface sinkholes, local depressions which were observed to appear over the tunnels as the machine advanced. In order to reconcile the different formats in which settlement values were reported for the NS-EW line and NEL and draw a meaningful comparison between the two, maximum values of settlement on the NS-EW line were compared with the depths of surface sinkholes which formed during NEL tunneling, since the latter is a measure of the maximum surface settlement experienced on the NEL (see Figure 4-1). For some cases, the depths of the surface sinkholes were not available and volumes of grout used to fill the sinkholes were indicated instead. As for the subsurface voids, the volumes of grout used to fill these voids were also included in Figure 4-1, though these voids were grouted before they could migrate to the surface

and did not actually result in surface settlements. As such, making the comparison between settlements on both lines comes with the following caveat: comparing exceptional cases of ground losses on the NEL with maximum settlements obtained during NS-EW tunneling makes perhaps an unfair comparison between what we know to be extreme cases of settlement on the NEL to what may be more indicative of average settlement values on the NS-EW line. Still, the comparison is useful even if only to demonstrate the scale of these large, localized ground losses experienced on the NEL to maximum settlements experienced on the NS-EW line. Figure 4-1 contains maximum surface settlements on the NS-EW line and NEL organized by MRT line, while Figure 4-2 presents the same information organized by geology.

4.1 Settlements in the Bukit Timah Granite

The Bukit Timah Granite is one of Singapore's underlying geological formations. Located in the central part of Singapore, encountering this formation is highly likely when tunneling across the island. Extensive weathering of this formation has occurred, resulting in large differences in engineering properties between different weathering grades of rock, and the creation of mixed faces of varying weathered grades of rock within the formation.

Settlements encountered in the Bukit Timah Granite are shown in Figure 4-3. During tunneling for the NS-EW line, construction methods employed included Greathead shields in both compressed and free air (data points 1, 2 and 3), TBMs in both compressed and free air (data points 4 and 5), and the New Austrian Tunneling Method (NATM) (data points 6 and 7). Settlements were well-controlled for all construction methods except for tunnels driven with the TBMs, in which over-excavation occurred when the volume of soil removed compared with the forward advance of the machine was not effectively controlled. While the use of compressed air to control face pressures resulted in significantly less settlement when the TBMs were used, the difference with the use of Greathead shields was insignificant.

EPB was first employed in this formation during NEL tunneling. Face pressures in the range of 0.4 to 0.6 times that of overburden pressures were found to be sufficient to control settlements in residual soil (Grade VI). In general, these face pressures are achieved in the residual soil, which had well-controlled settlements. However, the presence of mixed face conditions between different weathering grades of the Bukit Timah Granite made it difficult to sustain these face pressures, and large settlements occurred, including seven incidences of large, localized ground losses.

The seven incidences of large, localized ground losses which occurred during EPB tunneling in the Bukit Timah Granite consist of four incidences of surface sinkholes (data points 8 to 11 in Figure 4-3), and three subsurface voids (data points 12 to 14 in Figure 4-3). The depth of only one surface sinkhole is known and the magnitude of the other six ground losses are indicated only by the volume of grout used to fill them. While this makes it difficult to make a direct comparison with surface settlements, the large volumes of grout utilized to mitigate these ground losses speak for themselves. The reason for greater settlements experienced during tunneling in mixed grades of the Bukit Timah Granite lies in the different abilities of different weathered grades of the Bukit Timah Granite to form an adequate plug such that EPB is achieved during tunneling. Residual soil of Bukit Timah Granite (Grade VI) has high fines content and low permeability and is thus appropriate for EPB tunneling. However, the spoil of less weathered Bukit Timah Granite, i.e. moderately weathered Bukit Timah Granite (Grade III), has low fines content and consists mainly of gravel and cobble sized granite fragments, and as such cannot form an adequate plug, resulting in losses in face pressures. From Figure 4-3, in general, the settlements obtained during EPB tunneling on the NEL were greater than that obtained on the NS-EW line by tunneling with shields in free and compressed air and NATM.

During EPB tunneling, while settlement control in residual soil is good, settlement performance in the Bukit Timah Granite may be adverse if different weathering grades of the Bukit Timah Granite are encountered at the tunnel face. The high frequency of large, localized ground

losses encountered during EPB tunneling in these mixed face conditions in the Bukit Timah Granite seem to indicate that some caution should be exercised in employing EPB in the Bukit Timah Granite. A direct result of this experience on the NEL was to employ a greater number of slurry machines on the Circle Line (CCL), as slurry machines were judged to be less dependent on the properties of excavated spoil for face support. The result has had mixed success, since the occurrence of large, localized ground losses was not eliminated, and the additional problem of discharge of slurry to the surface was encountered. At the time of this writing, insufficient detailed information about the magnitudes of the settlements experienced on the CCL was available, so only a qualitative comparison can be made.

4.2 SETTLEMENTS IN THE JURONG FORMATION

The Jurong Formation, located in the western region of Singapore, is a sedimentary rock formation characterized by great variability in its engineering properties. This variability arises partly from the different strengths of component rocks, which is then compounded by different weathering extents in the component rocks. Tilting, folding and faulting in the Jurong Formation have created faulted zones which are an additional source of unpredictability in ground conditions during tunneling.

From Figure 4-4, settlements in the Jurong Formation were better controlled in shields with compressed air and with the use of NATM, as opposed to the use of shields in free air and EPB. Large settlements were encountered during both NS-EW line and NEL tunneling with the use of shields in free air because faulted zones and weathered rock were encountered in the tunnel face, and the lack of face support resulted in over-excavation. The decision not to employ face support when tunneling in (what has been judged to be) competent Jurong Formation rock may backfire and result in significantly large settlements if zones of faulted rock are encountered in the tunnel face.

In evaluating settlements for the NEL, Shirlaw, et al. (2003) differentiated between the Jurong Formation with overlying Kallang Formation and the Jurong Formation without overlying Kallang Formation to indicate differences in weathering extents of the Jurong Formation. The presence of valleys in the Jurong Formation which were subsequently infilled with the Kallang Formation signals the presence of zones of weaker rock or faulting/folding in the Jurong Formation (Shirlaw, et al., 2003). Settlements were uniformly low when tunneling using EPB in the Jurong Formation without overlying Kallang Formation, and were independent of face pressures applied. In this geology, one surface sinkhole (data point 10 on Figure 4-4) occurred during tunneling due to the breaking of an old water main as the tunnel face passed below it (Shirlaw, et al., 2001).

However, settlements in the Jurong Formation with overlying Kallang Formation were greater, not only in terms of relative volume losses, but also in the occurrence of large, localized ground losses. Five out of seven of these large, localized ground losses occurred during tunneling in this geology using EPB (data points 12 to 16 in Figure 4-4), while the remaining two occurred during launching/docking (data points 11 and 17 in Figure 4-4).

4.3 Settlements in the Kallang Formation

The Kallang Formation is largely located in the south-eastern portion of the island. Characterized by the presence of deformable, low strength marine clay, greater settlements in this formation are generally unsurprising. This was observed on the NS-EW line, where minimum settlements obtained in the Kallang Formation (about 20mm to 30mm) exceeded those obtained in the Bukit Timah Granite and the Jurong Formation (about 5mm to 10mm). On the NEL, greater values of Relative Volume Losses (RVL) were obtained in the Kallang Formation (about 5%) than in the Bukit Timah Granite and the Jurong Formation (about 2%).

With specific reference to construction methods employed in the Kallang Formation(Figure 4-5), the use of shields in compressed air and EPB on the NS-EW line resulted in more manageable

settlements (data points 1, 2, 3 and 6). Conversely, using shields in free air resulted in large settlements (datum point 4). Over-excavation occurred with the use of a TBM, even when compressed air was employed (datum point 5), which is similar to what occurred in the Bukit Timah Granite with the use of the TBM. EPB tunneling was deemed suitable to handle the marine clay of the Kallang Formation, and thus was adopted on the MRT network for the first time during tunneling on the NS-EW line. Second only to settlements induced by shields in compressed air (which were of 60mm to 100mm), EPB tunneling in the Kallang Formation was successful in controlling settlements (which was 120mm). This success was observed subsequently during tunneling on the NEL line. While relative volume losses in the Kallang Formation were greater than that in other formations, there were no incidences of large, localized ground losses during tunneling. An exceptionally large surface settlement occurred (data point 7 in Figure 4-5) during launching of the machine, with circumstances of that launch described in Section 3.3.4.3.

While EPB tunneling in the Kallang Formation alone was well-controlled, three large surface settlements occurred when mixed face conditions of the Jurong Formation and the Kallang Formation were encountered in the tunnel face (data points 8 to 10 of Figure 4-5). As the TBM drives from the stronger rock of the Jurong Formation to the soft ground of the Kallang Formation (or vice versa), operators can choose to apply face pressures in the range of 0.9 to 1.2 times that of overburden in order to control the soft ground in the Kallang Formation, though this may result in excessive heat and wear on the drill bits due to pressurized tunneling in the stronger material of the Jurong Formation. TBM operators hence have to consider this trade-off between settlement control and machine wear as they decide on face pressures to apply.

With the marine clay in the Kallang Formation, an additional concern for settlements is time-dependent consolidation settlement, which increased total settlement values on the NS-EW line during EPB tunneling four-fold.

4.4 Settlements in the Old Alluvium

The Old Alluvium occupies most of eastern Singapore, and consists of medium dense to very dense clayey coarse sand, fine gravel and lenses of silt and clay. Settlement during tunneling in the Old Alluvium was well-controlled on both the NS-EW line and NEL. From Figure 4-2, low settlements of 20mm were obtained during shield tunneling in compressed air on the NS-EW line (datum point 42). An incidence of a surface sinkhole occurred during docking of the machine during NEL tunneling (datum point 43). In terms of calculated relative volume losses during NEL tunneling, settlement was well-controlled with relative volume losses less than 2% for all surveyed points in the Old Alluvium.

4.5 Recommendations for Further Research

This thesis summarizes the background and performance of machine tunneling in the construction of Singapore's Mass Rapid Transit (MRT) network. In limiting the scope of the thesis to the MRT network, an interesting comparison with tunneling experience on the Deep Tunnel Sewerage Scheme (DTSS), in which large, localized ground losses were also experienced, was not made. DTSS tunnels, driven mainly using Earth Pressure Balance (EPB) machines, were generally at greater depths, and had smaller diameters, and thus could illustrate the influence of these two factors on settlement. While construction of the Changi Airport extension on the North-South East-West (NS-EW) line was mentioned in Chapter 1, delving into greater detail for that project may give interesting insights on the performance of EPB tunneling in the Old Alluvium, which was the main geological formation encountered. Given that construction on the Circle line (CCL) was recently completed, there are fewer papers which describe settlement encountered on the CCL as compared to those that describe settlement on older projects. This may change in the future, allowing for greater understanding of the impact of employing greater number of slurry machines on the CCL.

Settlement as a result of tunneling is an important measure of performance as it quantifies the risk tunneling poses to adjacent structures and activities. The complex interaction between geology and machine operation which influences settlement can only be described partially in a qualitative manner. Having identified factors which control settlement, the next step would lie in quantifying the magnitude of each factor's influence on settlement. This complex interaction is illustrated in findings by Suwansawat & Einstein (2006) in their analysis of factors such as tunnel geometry, geology and EPB shield operation parameters on surface settlement. They consistently found that surface settlements did not depend on individual factors, but on multiple parameters interacting with each other (Suwansawat & Einstein, 2006). To effectively model these complex relationships between influencing factors, artificial neural networks were used (Suwansawat & Einstein, 2006). A similar approach could be adopted specifically for Singapore's context.

At the time of writing, Singapore's transport minister had announced plans to double the length of Singapore's rail network by 2030 (Chow, 2013; Tan, 2013). This ambitious undertaking involves the extension of several existing lines and the construction of two new lines, the Cross Island line and Jurong Regional line, depicted in Figure 4-6 (Tan, 2013). Soil investigation works for the Cross Island line are slated to commence by mid-2013, and will involve the drilling of 70m deep boreholes every 15 to 20m along the tunnel alignment, to reduce uncertainty in characterizing ground conditions. The needs of a small city state and her ever-growing population have driven Singapore's civil engineers to continually search for ways to create space in an already land-scarce nation, by building higher or deeper. The need to understand how these construction projects will affect adjacent structures and surface activities remains just as important, if not more so.

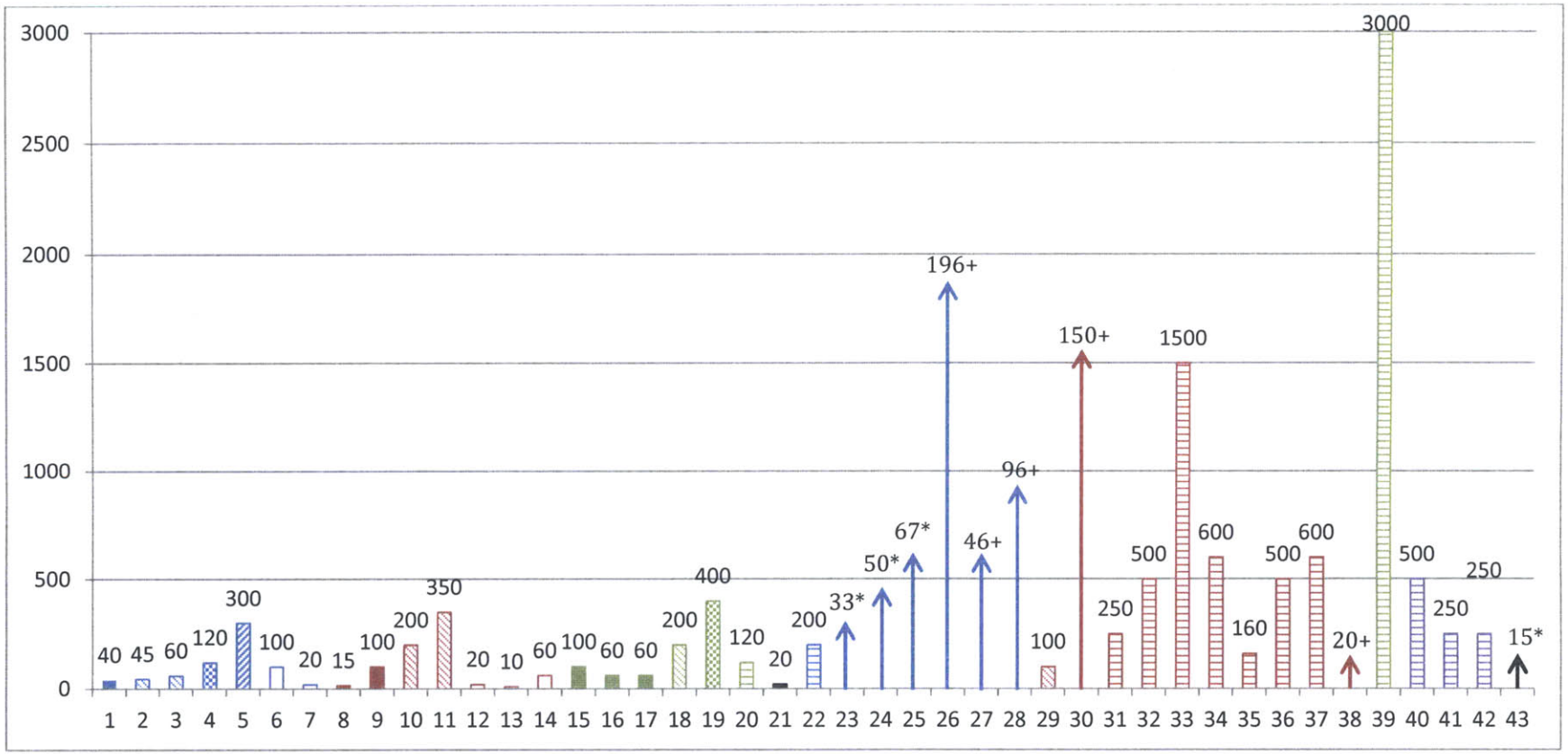

Figure 4-1: Maximum surface settlements on the North-South East-West line and North East line, organized by line (NS-EW line: data points 1 to 21; NEL: data points 22 to 43)

**Grout volumes of surface sinkholes (S) in m³; +Grout volumes of subsurface voids (V) in m³; data points 38, 39: settlements during launching; data points 32, 40, 43: settlements during docking; all other points: settlement during tunneling*

Legend *(more details on next page)*			
	Bukit Timah Granite		Shield in compressed air
	Jurong Formation		Shield in free air
	Kallang Formation		TBM in compressed air
	Mixed face: JF/KF		TBM in free air
	Old Alluvium		NATM
			EPB

	Line	Geology	Const. Method		Line	Geology	Const. Method
1	NS-EW	BTG	Shield in CA	22	NEL	BTG (GIII/GVI)	EPB (S)
2	NS-EW	BTG	Shield in FA	23	NEL	BTG (GIII/GVI)	EPB (S*)
3	NS-EW	BTG	Shield in FA	24	NEL	BTG (GIII/GVI)	EPB (S*)
4	NS-EW	BTG	TBM in CA	25	NEL	BTG (GIII/GVI)	EPB (S*)
5	NS-EW	BTG	TBM in FA	26	NEL	BTG (GIII)	EPB (V+)
6	NS-EW	BTG	NATM	27	NEL	BTG (GIII/GVI)	EPB (V+)
7	NS-EW	BTG	NATM	28	NEL	BTG (GIII/GVI)	EPB (V+)
8	NS-EW	JF	Shield in CA	29	NEL	JF (no KF above)	Shield in FA (S)
9	NS-EW	JF	Shield in CA	30	NEL	JF (no KF above)	Shield in FA (V+)
10	NS-EW	JF	Shield in FA	31	NEL	JF (no KF above)	EPB (S)
11	NS-EW	JF	Shield in FA	32	NEL	JF (KF above)	EPB (S)
12	NS-EW	JF	NATM	33	NEL	JF (KF above)	EPB (S)
13	NS-EW	JF	NATM	34	NEL	JF (KF above)	EPB (S)
14	NS-EW	JF	NATM	35	NEL	JF (KF above)	EPB (S)
15	NS-EW	KF	Shield in CA	36	NEL	JF (KF above)	EPB (S)
16	NS-EW	KF	Shield in CA	37	NEL	JF (KF above)	EPB (S)
17	NS-EW	KF	Shield in CA	38	NEL	JF (KF above)	EPB (V+)
18	NS-EW	KF	Shield in FA	39	NEL	KF	EPB (S)
19	NS-EW	KF	TBM in CA	40	NEL	JF/KF	EPB (S)
20	NS-EW	KF	EPB	41	NEL	JF/KF	EPB (S)
21	NS-EW	OA	Shield in CA	42	NEL	JF/KF	EPB (S)
				43	NEL	OA	EPB (S)

Line:
NS-EW: North-South East-West line
NEL: North-East line

Geology:
BTG: Bukit Timah Granite
GIII: moderately weathered BTG
GIII/GVI: mixed face between GIII and residual soil (GVI)
JF: Jurong Formation
KF: Kallang Formation
JF/KF: mixed face between JF and KF
OA: Old Alluvium

Construction method:
CA: Compressed air
FA: Free air
NATM: New Austrian Tunneling Method
EPB: Earth Pressure Balance
S: surface sinkhole
V: subsurface void
***/+:** only volumes of grout used available

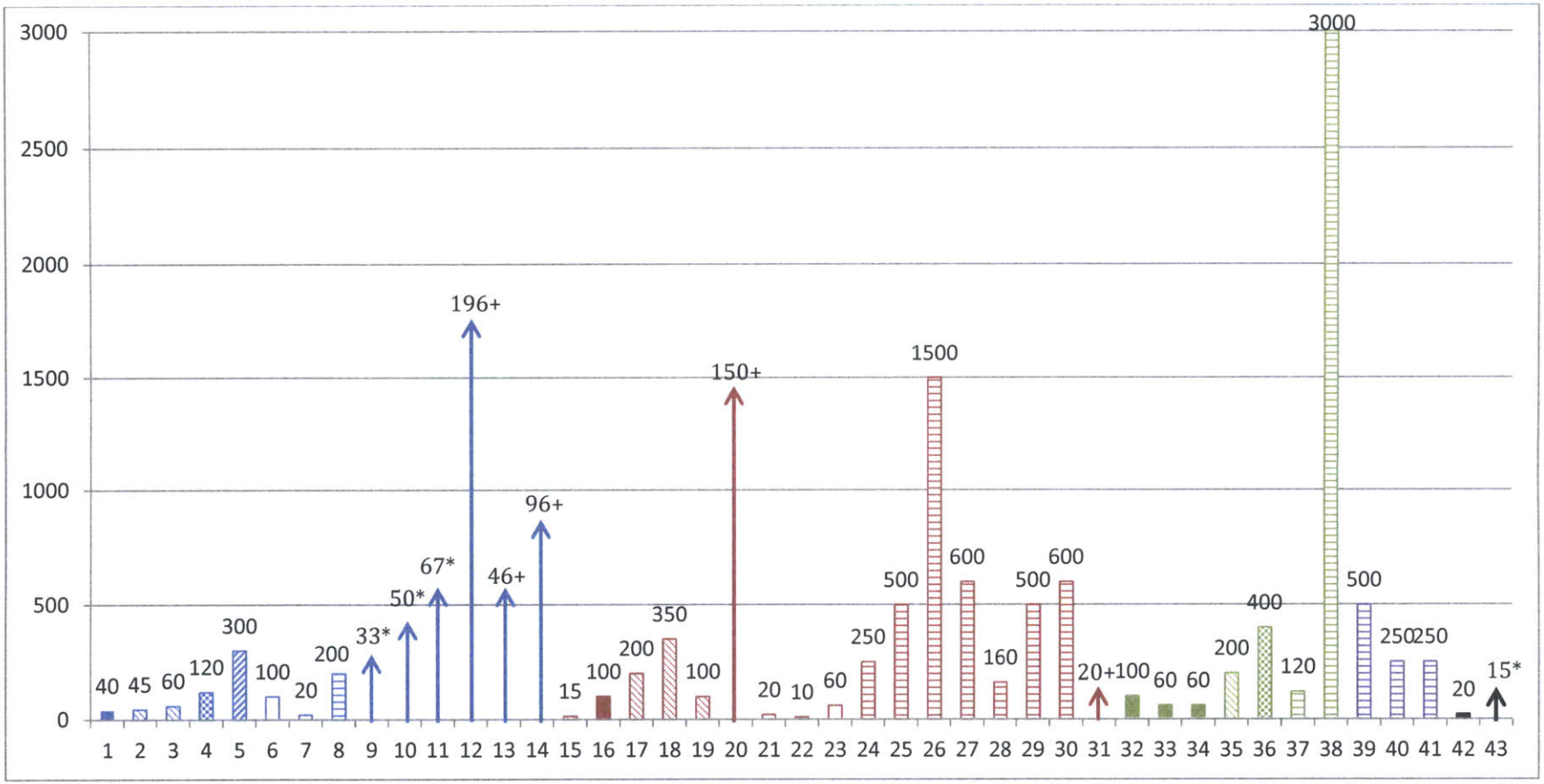

Figure 4-2: Maximum surface settlements on the North-South East-West line and North East line, organized by geology

**Grout volumes of surface sinkholes (S) in m³; +Grout volumes of subsurface voids (V) in m³; data points 31, 38: settlements during launching; data points 25, 39, 43: settlements during docking; all other points: settlement during tunneling*

Legend *(more details on next page)*			
	Bukit Timah Granite		Shield in compressed air
	Jurong Formation		Shield in free air
	Kallang Formation		TBM in compressed air
	Mixed face: JF/KF		TBM in free air
	Old Alluvium		NATM
			EPB

	Line	Geology	Const. Method		Line	Geology	Const. Method
1	NS-EW	BTG	Shield in CA	*22*	NEL	JF (no KF above)	Shield in FA (S)
2	NS-EW	BTG	Shield in FA	*23*	NEL	JF (no KF above)	Shield in FA (V+)
3	NS-EW	BTG	Shield in FA	*24*	NEL	JF (no KF above)	EPB (S)
4	NS-EW	BTG	TBM in CA	*25*	NEL	JF (KF above)	EPB (S)
5	NS-EW	BTG	TBM in FA	*26*	NEL	JF (KF above)	EPB (S)
6	NS-EW	BTG	NATM	*27*	NEL	JF (KF above)	EPB (S)
7	NS-EW	BTG	NATM	*28*	NEL	JF (KF above)	EPB (S)
8	NEL	BTG (GIII/GVI)	EPB (S)	*29*	NEL	JF (KF above)	EPB (S)
9	NEL	BTG (GIII/GVI)	EPB (S*)	*30*	NEL	JF (KF above)	EPB (S)
10	NEL	BTG (GIII/GVI)	EPB (S*)	*31*	NEL	JF (KF above)	EPB (V+)
11	NEL	BTG (GIII/GVI)	EPB (S*)	*32*	NS-EW	KF	Shield in CA
12	NEL	BTG (GIII)	EPB (V+)	*33*	NS-EW	KF	Shield in CA
13	NEL	BTG (GIII/GVI)	EPB (V+)	*34*	NS-EW	KF	Shield in CA
14	NEL	BTG (GIII/GVI)	EPB (V+)	*35*	NS-EW	KF	Shield in FA
15	NS-EW	JF	Shield in CA	*36*	NS-EW	KF	TBM in CA
16	NS-EW	JF	Shield in CA	*37*	NS-EW	KF	EPB
17	NS-EW	JF	Shield in FA	*38*	NEL	KF	EPB (S)
18	NS-EW	JF	Shield in FA	*39*	NEL	JF/KF	EPB (S)
19	NS-EW	JF	NATM	*40*	NEL	JF/KF	EPB (S)
20	NS-EW	JF	NATM	*41*	NEL	JF/KF	EPB (S)
21	NS-EW	JF	NATM	*42*	NS-EW	OA	Shield in CA
				43	NEL	OA	EPB (S)

Line:
NS-EW: North-South East-West line
NEL: North-East line

Geology:
BTG: Bukit Timah Granite
GIII: moderately weathered BTG
GIII/GVI: mixed face between GIII and residual soil (GVI)
JF: Jurong Formation
KF: Kallang Formation
JF/KF: mixed face between JF and KF
OA: Old Alluvium

Construction method:
CA: Compressed air
FA: Free air
NATM: New Austrian Tunneling Method
EPB: Earth Pressure Balance
S: surface sinkhole
V: subsurface void
***/+:** only volumes of grout used available

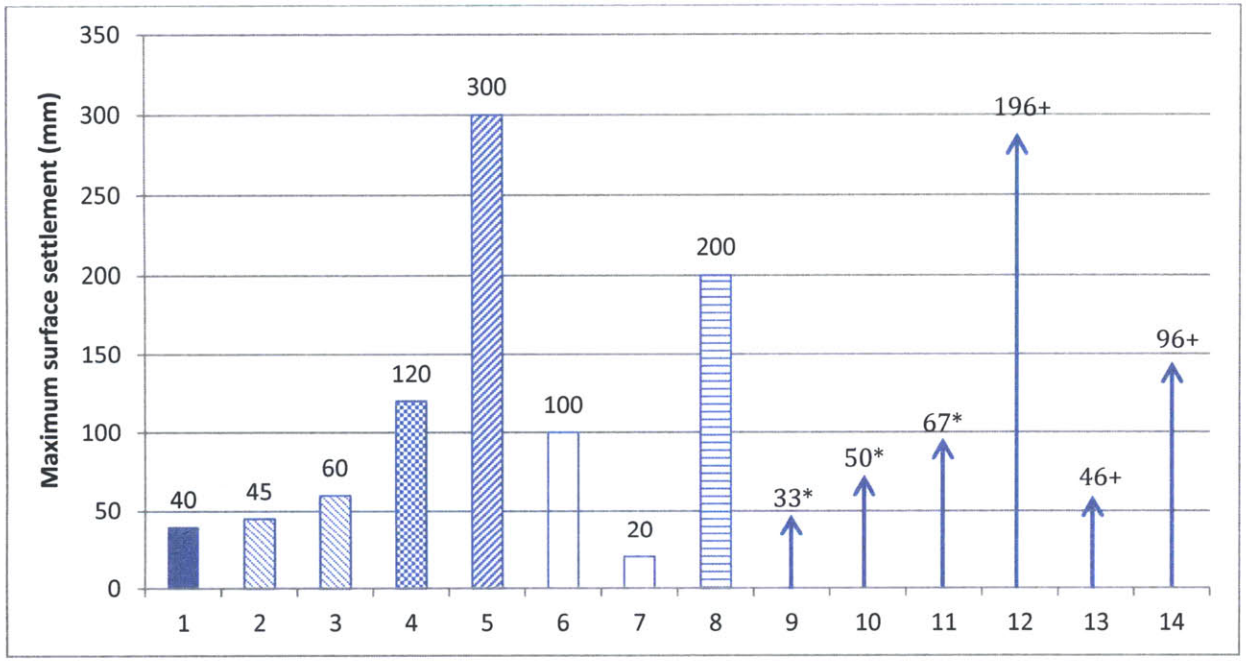

	Line	Geology	Const. Method
1	NS-EW	BTG	Shield in CA
2	NS-EW	BTG	Shield in FA
3	NS-EW	BTG	Shield in FA
4	NS-EW	BTG	TBM in CA
5	NS-EW	BTG	TBM in FA
6	NS-EW	BTG	NATM
7	NS-EW	BTG	NATM
8	NEL	GIII/GVI	EPB (S)
9	NEL	GIII/GVI	EPB (S*)
10	NEL	GIII/GVI	EPB (S*)
11	NEL	GIII/GVI	EPB (S*)
12	NEL	GIII	EPB (V+)
13	NEL	GIII/GVI	EPB (V+)
14	NEL	GIII/GVI	EPB (V+)

Figure 4-3: Maximum surface settlements on the North-South East-West line and North East line for the Bukit Timah Granite, organized by construction method

**Grout volumes of surface sinkholes (S) in m³;*
+Grout volumes of subsurface voids (V) in m³

Legend	
	Shield in compressed air
	Shield in free air
	TBM in compressed air
	TBM in free air
	NATM
	EPB

Line:	**NS-EW:** North-South East-West line **NEL:** North-East line
Geology:	**BTG:** Bukit Timah Granite **GIII:** moderately weathered BTG **GIII/GVI:** mixed face between moderately weathered BTG and residual soil **JF:** Jurong Formation **KF:** Kallang Formation **JF/KF:** mixed face between JF and KF **OA:** Old Alluvium
Construction method:	**CA:** Compressed air **FA:** Free air **NATM:** New Austrian Tunneling Method **EPB:** Earth Pressure Balance **S:** surface sinkhole **V:** subsurface void ***/+:** only volumes of grout used available

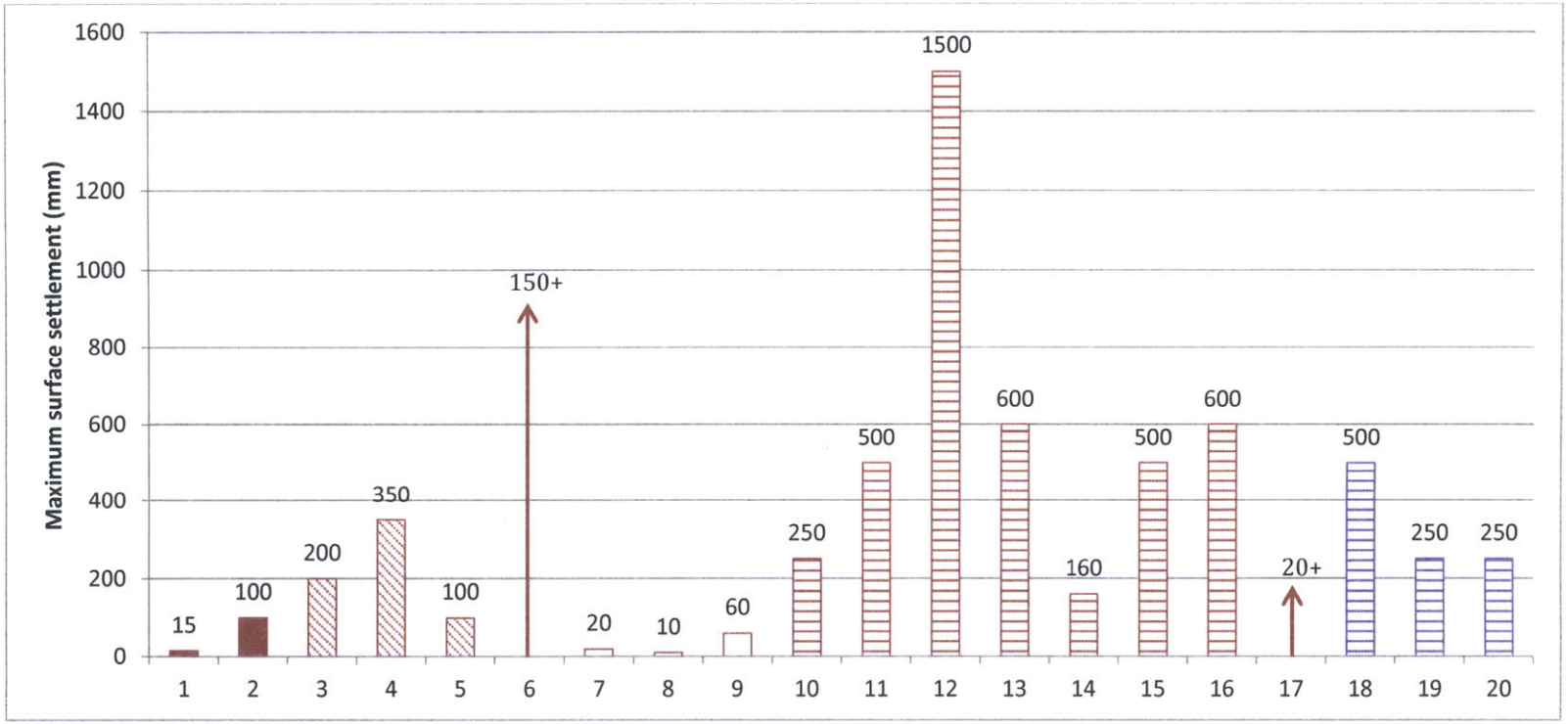

Figure 4-4: Maximum surface settlements on the North-South East-West line and North East line for the Jurong Formation, organized by construction method

**Grout volumes of surface sinkholes (S) in m^3;*

+Grout volumes of subsurface voids (V) in m^3;

Datum point 17: settlement during launching;

Datum point 11: settlements during docking;

All other points: settlement during tunneling

	Line	Geology	Const. Method
1	NS-EW	JF	Shield in CA
2	NS-EW	JF	Shield in CA
3	NS-EW	JF	Shield in FA
4	NS-EW	JF	Shield in FA
5	NEL	JF (no KF above)	Shield in FA
6	NEL	JF (no KF above)	Shield in FA (V+)
7	NS-EW	JF	NATM
8	NS-EW	JF	NATM
9	NS-EW	JF	NATM
10	NEL	JF (no KF above)	EPB (S)
11	NEL	JF (KF above)	EPB (S)
12	NEL	JF (KF above)	EPB (S)
13	NEL	JF (KF above)	EPB (S)
14	NEL	JF (KF above)	EPB (S)
15	NEL	JF (KF above)	EPB (S)
16	NEL	JF (KF above)	EPB (S)
17	NEL	JF (KF above)	EPB (V+)
18	NEL	JF/KF	EPB (S)
19	NEL	JF/KF	EPB (S)
20	NEL	JF/KF	EPB (S)

Legend	
	Shield in compressed air
	Shield in free air
	TBM in compressed air
	TBM in free air
	NATM
	EPB

Line:
- **NS-EW:** North-South East-West line
- **NEL:** North-East line

Geology:
- **BTG:** Bukit Timah Granite
- **GIII:** moderately weathered BTG
- **GIII/GVI:** mixed face between moderately weathered BTG and residual soil
- **JF:** Jurong Formation
- **KF:** Kallang Formation
- **JF/KF:** mixed face between JF and KF
- **OA:** Old Alluvium

Construction method:
- **CA:** Compressed air
- **FA:** Free air
- **NATM:** New Austrian Tunneling Method
- **EPB:** Earth Pressure Balance
- **S:** surface sinkhole
- **V:** subsurface void
- ***/+:** only volumes of grout used available

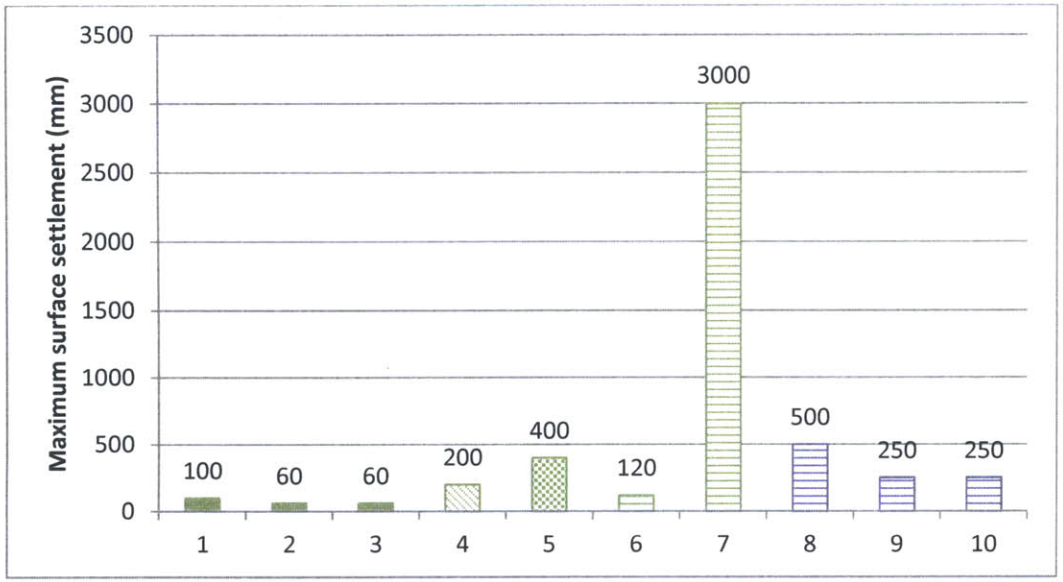

	Line	Geology	Const. Method
1	NS-EW	KF	Shield in CA
2	NS-EW	KF	Shield in CA
3	NS-EW	KF	Shield in CA
4	NS-EW	KF	Shield in FA
5	NS-EW	KF	TBM in CA
6	NS-EW	KF	EPB
7	NEL	KF	EPB (S)
8	NEL	JF/KF	EPB (S)
9	NEL	JF/KF	EPB (S)
10	NEL	JF/KF	EPB (S)

Figure 4-5: Maximum surface settlements on the North-South East-West line and North East line for the Kallang Formation, organized by construction method

Datum point 7: settlement during launching; all other points: settlement during tunneling

Legend	
	Shield in compressed air
	Shield in free air
	TBM in compressed air
	TBM in free air
	NATM
	EPB

Line:	**NS-EW:** North-South East-West line **NEL:** North-East line
Geology:	**BTG:** Bukit Timah Granite **GIII:** moderately weathered BTG **GIII/GVI:** mixed face between moderately weathered BTG and residual soil **JF:** Jurong Formation **KF:** Kallang Formation **JF/KF:** mixed face between JF and KF **OA:** Old Alluvium
Construction method:	**CA:** Compressed air **FA:** Free air **NATM:** New Austrian Tunneling Method **EPB:** Earth Pressure Balance **S:** surface sinkhole **V:** subsurface void ***/+:** only volumes of grout used available

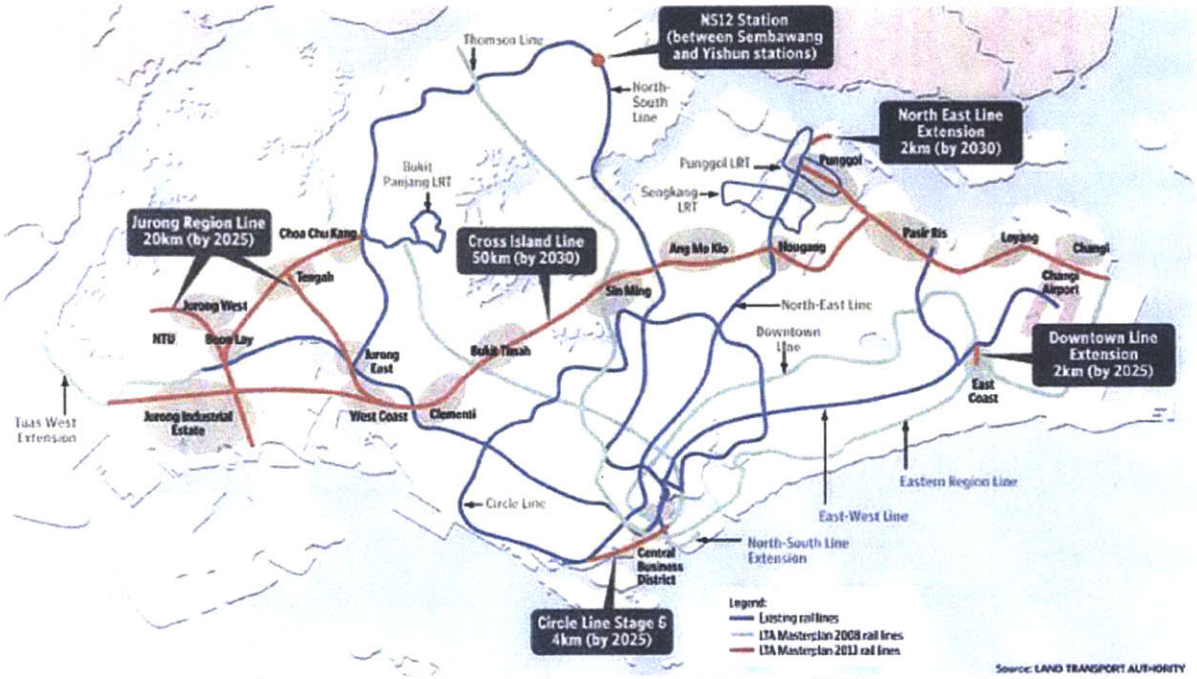

Figure 4-6: Proposed extension of Singapore's Mass Rapid Transit (MRT) network (Tan, 2013)

BIBLIOGRAPHY

Balasubramaniam, K., & Musa, M. A. (1993). Mechanised Shields for Trenchless Sewer Construction in Singapore. *Proceedings of VIII Australian Tunnelling Conference, Sydney, Australia*.

Bieniawski, Z. T. (1984). *Rock Mechanics Design in Mining and Tunneling*. Rotterdam: A. A. Balkema.

Bonnett, C. F. (2005). Practical Railway Engineering. London: Imperial College Press.

BSI. (1999). BS5930: 1999 Code of practice for site investigations. *Section 6: Description of soils and rocks.* London: British Standards Institution.

Chow, J. (2013). Studies for Cross Island Line to start, *The Straits Times*. Retrieved from http://www.straitstimes.com/breaking-news/singapore/story/studies-cross-island-line-start-20130506

DSTA. (2009). *Geology of Singapore*. Singapore: Defence Science & Technology Agency.

Hulme, T. W., & Burchell, A. J. (1992). Bored Tunneling for Singapore Metro. *Journal of Construction Engineering and Management-ASCE, 118*(2), 363-384.

Hulme, T. W., & Burchell, A. J. (1999). Tunnelling projects in Singapore: an overview. *Tunnelling and Underground Space Technology, 14*(4), 409-418.

Lane, K. S. (2013). tunnels and underground excavations. *Encyclopædia Britannica*. Retrieved from http://www.britannica.com/EBchecked/topic/609297/tunnel

LTA. (2010). E/GD/09/106/A1 Civil Design Criteria for Road and Rail Transit Systems. *Chapter 5: Geotechnical Parameters.* Singapore: Land Transport Authority.

Maidl, B., Herrenknecht, M., & Anheuser, L. (1996). *Mechanised Shield Tunnelling*. Berlin: Ernst and Sohn.

Maidl, B., Schmid, L., Ritz, W., & Herrenknecht, M. (2008). *Hardrock Tunnel Boring Machines*: Ernst and Sohn.

Mair, R. J., Taylor, R. N., & Bracegirdle, A. (1993). Subsurface settlement profiles above tunnels in clays. *Geotechnique, 42*(2), 315-320.

Moores, E. M., & Fairbridge, R. W. (1997). *Encyclopedia of European and Asian regional geology*. London: Chapman & Hall.

Osborne, N. H., Knight-Hassell, C. K., Tan, L. C., & Wong, R. (2008). A review of the performance of the tunnelling for Singapore's circle line project. *Proceedings of World Tunnel Congress - Underground Facilities for Better Environment and Safety, India*, 1497-1508.

Ow, C. N., Kulaindran, A., Knight-Hassell, C. K., & Seah, T. P. (2004). Progress of Rail (Metro) Tunnel Construction in Singapore - Past, Present & Future. *Tunnelling and Underground Space Technology. Proceedings of 30th ITA-AITES World Tunnel Congress, 19*.

Pitts, J. (1984). A Review of Geology and Engineering Geology in Singapore. *Quarterly Journal of Engineering Geology, 17*(2), 93-101.

Reilly, B. J. (1999). EPBMs for the North East Line Project. *Tunnelling and Underground Space Technology, 14*(4), 18.

Sharma, J. S., Chu, J., & Zhao, J. (1999). Geological and Geotechnical Features of Singapore: an overview. *Tunnelling and Underground Space Technology, 14*(4), 419-431.

Shirlaw, J. N., Boone, S. J., Sugden, N. B., & Peach, A. (2005). Controlling the risk of sinkholes over EPB driven tunnels - a client perspective. *Proceedings of Geotechnical Aspects of Underground Construction in Soft Ground, Amsterdam, the Netherlands*. doi: 10.1201/NOE0415391245.ch59

Shirlaw, J. N., Hencher, S. R., & Zhao, J. (2000). Design and construction issues for excavation and tunnelling in some tropically weathered rocks and soils. *Proceedings of GeoEng 2000, Melbourne, Australia, 1*, 1286-1329.

Shirlaw, J. N., & Hulme, T. W. (2008). Risk mitigation for slurry TBMs. *Tunnels & Tunnelling International, 4*, 26-28.

Shirlaw, J. N., & Hulme, T. W. (2011). Marrying Risk Management to Slurry TBM Construction. Retrieved from STEC TUNNELweb website: http://english.stec.net/english/english_detail.asp?id=815

Shirlaw, J. N., Ong, J. C. W., Rosser, H. B., Osborne, N. H., Tan, C. G., & Heslop, P. J. E. (2001). Immediate settlements due to tunnelling for the North East Line. *Proceedings of Underground Singapore, Singapore*, 76-90.

Shirlaw, J. N., Ong, J. C. W., Rosser, H. B., Tan, C. G., Osborne, N. H., & Heslop, P. J. E. (2003). Local settlements and sinkholes due to EPB tunnelling. *Geotechnical Engineering, 156*(GE4).

Sousa, R. L. (2010). *Risk Analysis for Tunneling Projects (doctoral dissertation).* Massachusetts Institute of Technology, Cambridge, MA.

Suwansawat, S. (2002). *Earth Pressure Balance (EPB) Shield Tunneling in Bangkok: Ground Response and Prediction of Surface Settlements Using Artificial Neural Networks (doctoral dissertation).* Massachusetts Institute of Technology, Cambridge, MA.

Suwansawat, S., & Einstein, H. H. (2006). Artificial neural networks for predicting the maximum surface settlement caused by EPB shield tunneling. *Tunnelling and Underground Space Technology, 21*, 133-150.

Tan, C. (2013). More new MRT lines to be built by 2030, *The Straits Times*. Retrieved from http://www.straitstimes.com/breaking-news/singapore/story/more-new-mrt-lines-be-built-2030-20130117

Zhao, J. (2012). *A General Overview of Tunnel Boring Machines* [Powerpoint Slides]. Retrieved from http://www.ncus.ntu.edu.sg/Events/Documents/SRMEG%20Seminar%20Tunnel%20Boring%20Machines.pdf